AD-A163 523 CHARACTERISTIC MODES FOR A SLOT IN A CONDUCTING PLANE (U) SYRACUSE UNIV NY DEPT OF ELECTRICAL AND COMPUTER ENGINEERING K Y KABALAN ET AL. DEC 85 SYRU/DECE/TR85/6 1/2

UNCLASSIFIED N00014-85-K-0082 F/G 20/3 NL

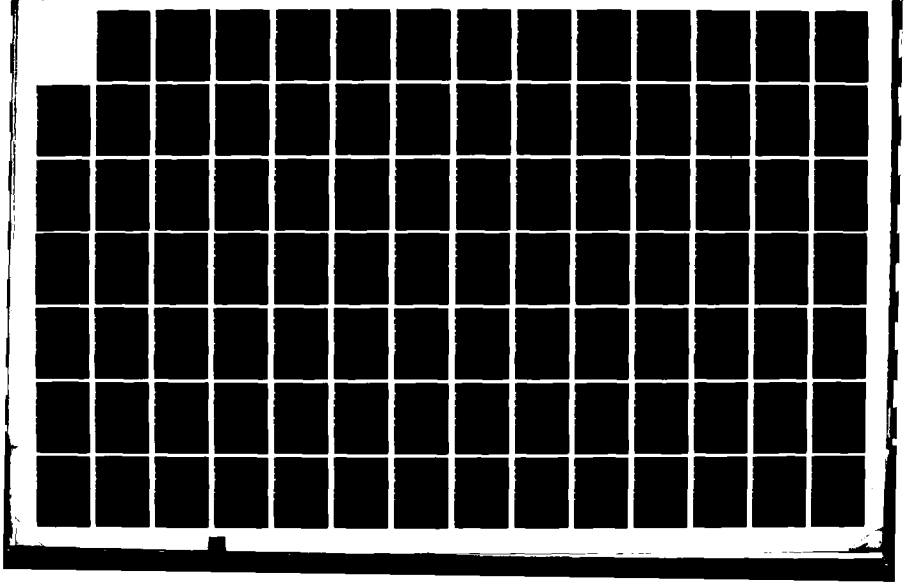

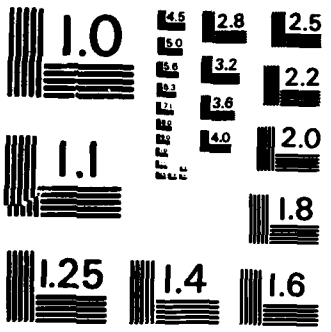

MICROCOPY RESOLUTION TEST CHART
NATIONAL BUREAU OF STANDARDS-1963-A

SYRU/DECE/TR-85/6

CHARACTERISTIC MODES FOR A SLOT IN A CONDUCTING PLANE

by

[illegible]

[illegible]

[illegible] 1985

[illegible] N00014-85-C-0082

[illegible]

SYRU/DECE/TR-85/6

CHARACTERISTIC MODES FOR A SLOT IN A CONDUCTING PLANE

by

Karim Y. Kabalan
Roger F. Harrington
Joseph R. Mautz

Department of
Electrical and Computer Engineering
Syracuse University
Syracuse, New York 13210

Technical Report No. 2

December 1985

Contract No. N00014-85-K-0082

Approved for public release; distribution unlimited

Prepared for

DEPARTMENT OF THE NAVY
OFFICE OF NAVAL RESEARCH
ARLINGTON, VIRGINIA 22217

UNCLASSIFIED

SECURITY CLASSIFICATION OF THIS PAGE (When Data Entered)

REPORT DOCUMENTATION PAGE		READ INSTRUCTIONS BEFORE COMPLETING FORM
1. REPORT NUMBER SYRU/DECE/TR-85/6	2. GOVT ACCESSION NO. A163523	3. RECIPIENT'S CATALOG NUMBER
4. TITLE (and Subtitle) CHARACTERISTIC MODES FOR A SLOT IN A CONDUCTING PLANE		5. TYPE OF REPORT & PERIOD COVERED Technical Report No. 2 6. PERFORMING ORG. REPORT NUMBER
7. AUTHOR(s) Karim Y. Kabalan Roger F. Harrington Joseph R. Mautz		8. CONTRACT OR GRANT NUMBER(s) N00014-85-K-0082
9. PERFORMING ORGANIZATION NAME AND ADDRESS Dept. of Electrical & Computer Engineering Syracuse University Syracuse, New York 13210		10. PROGRAM ELEMENT, PROJECT, TASK AREA & WORK UNIT NUMBERS
11. CONTROLLING OFFICE NAME AND ADDRESS Department of the Navy Office of Naval Research Arlington, Virginia 22217		12. REPORT DATE December 1985 13. NUMBER OF PAGES 108
14. MONITORING AGENCY NAME & ADDRESS(if different from Controlling Office)		15. SECURITY CLASS. (of this report) UNCLASSIFIED 15a. DECLASSIFICATION/DOWNGRADING SCHEDULE

16. DISTRIBUTION STATEMENT (of this Report)

Approved for public release; distribution unlimited.

17. DISTRIBUTION STATEMENT (of the abstract entered in Block 20, if different from Report)

18. SUPPLEMENTARY NOTES

19. KEY WORDS (Continue on reverse side if necessary and identify by block number)

Aperture admittance
Characteristic modes
Electromagnetic transmission
Slot in a plane
Two-dimensional slot

20. ABSTRACT (Continue on reverse side if necessary and identify by block number)

In this report, the theory of characteristic modes for slots is used to solve the problem of an infinitely long slot in a conducting plane in an unbounded medium illuminated by either a transverse electric or a transverse magnetic uniform plane wave. The characteristic currents are defined as the eigenfunctions of a certain generalized eigenvalue equation involving the admittance operator and its real part. The theory is general, applicable to wide as well as narrow slots, and gives a modal expansion of all

DD FORM 1 JAN 73 1473 EDITION OF 1 NOV 65 IS OBSOLETE
S/N 0102-014-6601

UNCLASSIFIED

SECURITY CLASSIFICATION OF THIS PAGE (When Data Entered)

20. Abstract (continued)

quantities and parameters of interest usually encountered in electromagnetic compatibility problems. This modal expansion converges rapidly when the slot is narrow. The characteristic currents and fields, the equivalent magnetic current, and the radiation pattern are computed for different slot widths. Analytic expressions for the special case of a narrow slot are also given.

CONTENTS

CHAPTER 1

INTRODUCTION

The problem of electromagnetic coupling from one region to another region through an aperture in a conducting plane can be formulated in terms of two admittance operators, one for each region [1]. These admittance operators are complex and symmetric. Recently, a theory for the characteristic modes for apertures has been proposed [2]. The characteristic currents are defined as the eigenfunctions of a certain generalized eigenvalue equation involving the admittance operators and their real parts. Because of the particular choice of the eigenvalue equation, the characteristic currents are real (or equiphase) and orthogonal with respect to the admittance operator, its real part, and its imaginary part over the aperture. Furthermore, the characteristic fields produced by the characteristic currents are orthogonal over the radiation sphere. For small apertures, the characteristic mode theory reduces to an augmented Bethe hole theory, i.e., the aperture is described by a susceptance term related to the polarizability, plus a conductance term.

Of aperture problems, the problem of an infinitely long slot in a conducting plane (see Figure 1-1) has been

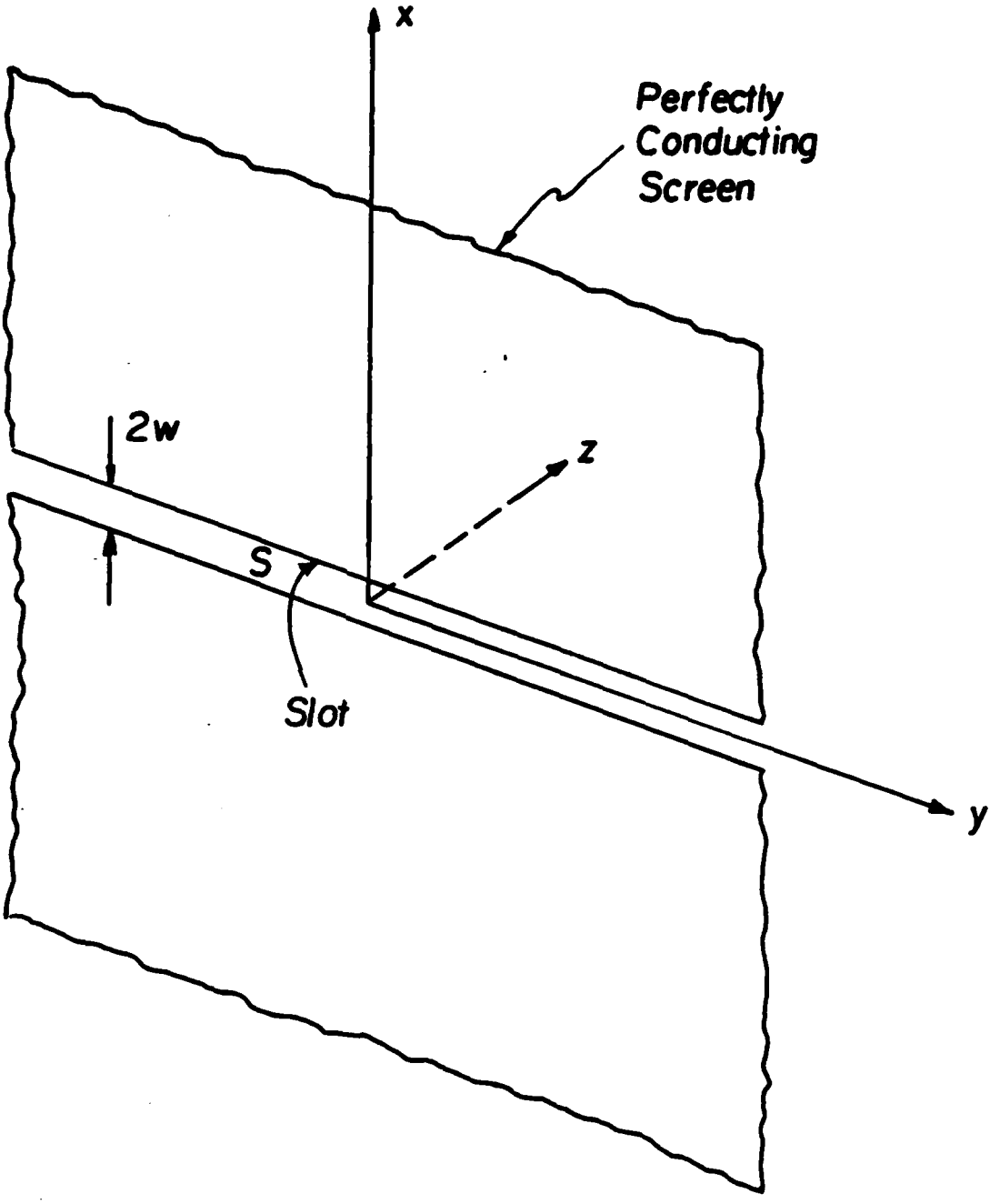

Figure 1-1. An infinitely long slot in a conducting plane.

considered most over the years since it was first addressed by Lord Rayleigh [3]. In his solution, Lord Rayleigh relied on reducing the problem to known solutions of hydrodynamic or electrostatic problems, but treated only the special case of a sufficiently narrow slot (a slit) [4, Page 273]. The narrow slot has since continued to receive particular attention. Morse and Rubenstein [5] provided an exact solution for the slit. Their analysis was based on solving the Helmholtz equation in elliptic coordinates using separation of variables, and, as a result, involved series of Mathieu functions. Later, Barakat [6] generalized their work to a slot in a conducting plane separating mediums with different electromagnetic properties. Sommerfeld [4, Section 39] reduced the associated boundary value problem into an integral equation for the electric field in the slot for uniform transverse electric and magnetic plane waves normally incident on the slot. Although the formulation is general and valid for wide slots of arbitrary width, the solution was given only under narrow slot approximations. Millar [7], extending Sommerfeld's equations to obliquely incident plane waves, solved for the electric field in the slot in the form of a power series in the ratio of slot width to wavelength. Houlberg [8] then generalized the work of Millar to the two-medium

problem. Variational techniques [9, Section 7-12] also found their application to the solution of narrow slots. More recently, Butler and Wilton [10] used a series expansion of Chebyshev polynomials to obtain exact solutions for the equivalent magnetic current on the narrow slot for a general excitation.

Effective solutions for wide slots of width comparable to the wavelength, however, have only become possible with the advance of solution techniques based on the method of moments [11]. Typically, an operator, usually integral, equation is derived for some unknown parameter from which all other quantities can be derived. As in narrow slot solutions, the unknown parameter is approximated by a linear combination of some known functions, but, in contrast to narrow slot solutions, the kernel of the integral equation is not replaced by its small argument approximation. The inner products of the integral equation with testing functions form a matrix equation whose solution determines the unknown coefficients. Butler and Umashankar [12] utilized the generalized admittance formulation to solve the two-medium problem. Chou and Adams [13] treated single and double slots in an unbounded medium by converting the slot problem to that of a strip using Babinet's principle [9, Section 7-12]. Other varieties of

slot problems were also considered. Lewis [14] studied the effect of covering the slot by a dielectric sheath, while Nevels and Butler [15] solved the problem of a slot in a ground screen covered by a dielectric slab. Electromagnetic transmission through a filled slot in a thick conducting plane was investigated by Auckland and Harrington [16], [17].

In this report, the theory of characteristic modes for apertures is specialized to an infinitely long slot in a conducting plane in an unbounded medium. The theory is then applied to a complete solution of the slot problem when the slot is illuminated by

1- a uniform transverse electic (to the slot axis) plane wave,
2- a uniform tranverse magnetic (to the slot axis) plane wave.

Specifically, the characteristic currents and field modes are computed for different slots. These are then used to compute the quantities and parameters of importance usually encountered in electromagnetic field compatibility problems, such as the equivalent magnetic current of the slot, the transmission coefficient, and transmitted field pattern far from the slot. Analytic expressions for the special case of the narrow slot are also given. It is

shown that the theory of characteristic modes is a very useful theoretical tool. It allows for a modal expansion of all quantities of interest, and can be applied to narrow slots as well as to general slots of arbitrary width. Furthermore, it is shown that it is computationally very efficient. It exhibits features and speed of convergence that make it more attractive than many other numerical solutions.

The theory of characteristic modes is applied in the report only to a slot in a conducting plane in an unbounded medium. Such a restriction is not essential, and is intended only to simplify the theory. The extension to the two-medium problem is straightforward, and can be accomplished with a few obvious changes in the present analysis. The conclusions drawn here for the one-medium problem are expected to hold for the two-medium problem. Finally, a word about the organization of the report is in order. In Chapter 2, the theory of characteristic modes for a slot in a conducting plane in an unbounded medium is presented. In Chapters 3 and 4, the theory of characteristic modes is applied to transverse electric and magnetic plane wave excitations of the slot, respectively. In Chapter 5, conclusions are drawn and some final remarks are given.

CHAPTER 2

THE CHARACTERISTIC MODES FOR A SLOT IN A CONDUCTING PLANE

The characteristic currents and fields for a slot in a conducting plane in an unbounded medium are defined in this chapter. The characteristic currents are the solutions of an eigenvalue equation relating the tangential components of the magnetic field at the slot. The characteristic fields are the fields produced by the characteristic currents on the slot in the presence of the complete screen. These currents and field modes are then used for the solution of the slot problem. A Galerkin solution of the eigenvalue equation is given at the end of the chapter.

2-1 Derivation of the Operator Equation

Let the excitation of the slot be a field ($\underline{E}^a$, $\underline{H}^a$) incident from the left of the screen ($z<0$). This field is called the incident field. It is the field that would exist if the conducting screen were absent. Because of the presence of the screen with the slot, part of the incident field is reflected back, while the rest is transmitted into the $z>0$ half-space. The total field, incident plus scattered, ($\underline{E}$, $\underline{H}$), must have zero electric field component tangent to the screen, and continuous tangential electric and magnetic fields across the slot. Below, a field

equivalence theorem is used to divide the problem into two decoupled parts.

Let the exciting field be incident while the slot is covered by a perfect conductor. This field, often referred to as the short-circuit field, is denoted ($\underline{E}^{sc}$, $\underline{H}^{sc}$). By the field equivalence theorem [9, Section 3-5], the field to the left of the screen is identical with ($\underline{E}^{sc}$, $\underline{H}^{sc}$) plus the field ($\underline{E}(\underline{M})$, $\underline{H}(\underline{M})$) produced by the magnetic current sheet

$$\underline{M} = \underline{u}_z \times \underline{E}\Big|_{z=0} \tag{2-1}$$

on the slot while it is covered by a perfect conductor. The field to the right of the screen is then identical with the field ($\underline{E}(-\underline{M})$, $\underline{H}(-\underline{M})$) produced by the magnetic current sheet $-\underline{M}$ on the slot while it is covered by a perfect conductor. Figure 2-1 shows the equivalent situations.

The total tangential electric field clearly vanishes at the conducting screen. Furthermore, the tangential electric field is continuous across the slot by virtue of placing magnetic current sheets of opposite signs on the opposite sides of the slot. The continuity of the magnetic field across the slot, however, requires that

$$\underline{H}_t(\underline{M}) + \underline{H}_t^{sc} = \underline{H}_t(-\underline{M}) = -\underline{H}_t(\underline{M}). \tag{2-2}$$

In (2-2), the subscript t refers to the tangential component, and the last equality follows because of the

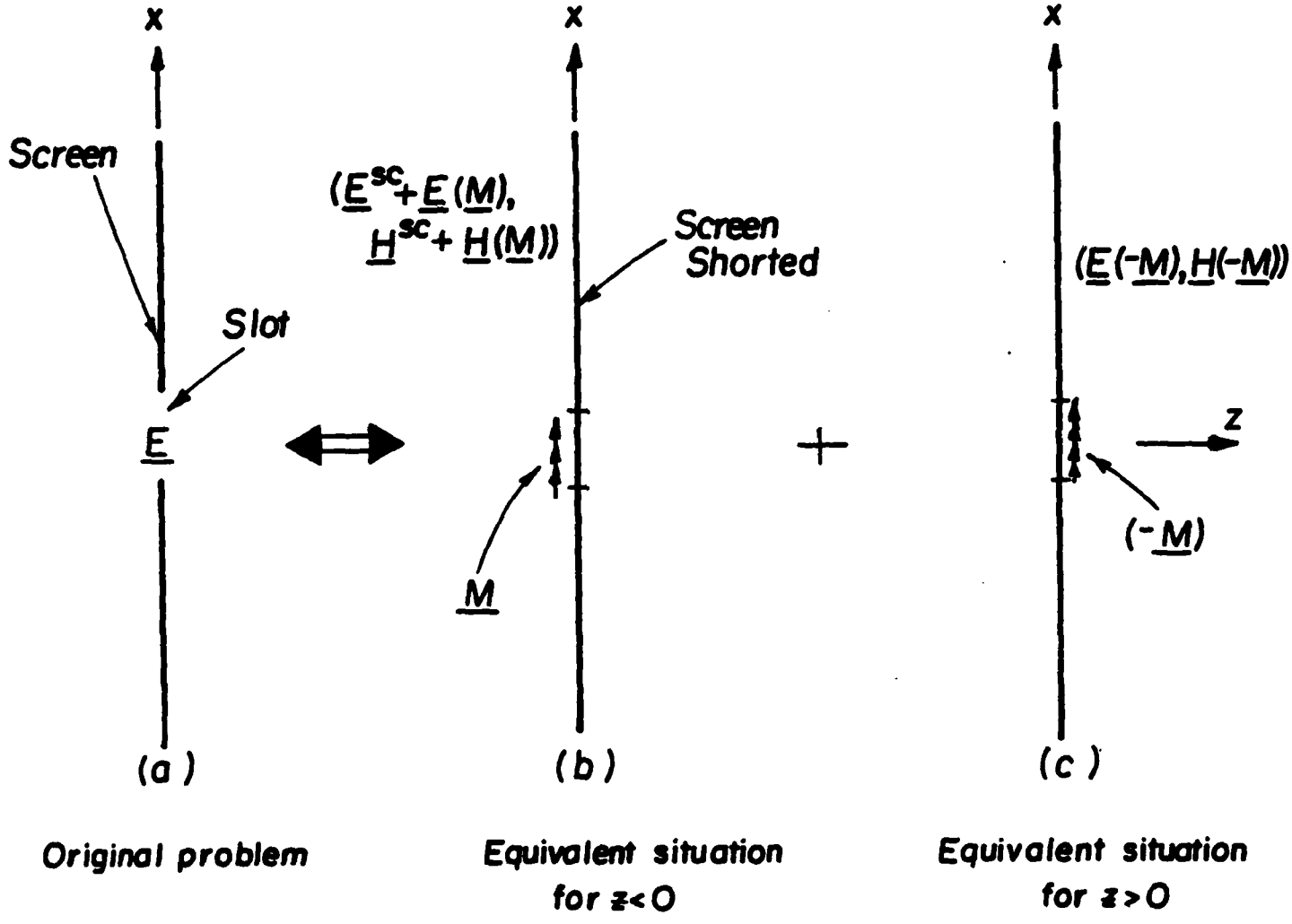

Figure 2-1. The equivalent situations.

linearity of the magnetic field. Rearranging, (2-2) then becomes

$$-2\,\underline{H}_e(M) = \underline{H}_e^{inc}. \tag{2-3}$$

In the next section, the characteristic currents of the slot are defined. These currents are then utilized to solve (2-3) for $\underline{M}$.

2-2 The Characteristic Currents of the Slot

The operator equation (2-3) can be rewritten in the form

$$\underline{Y}(\underline{M}) = \underline{I} \tag{2-4}$$

where

$$\underline{Y}(\underline{M}) = -2\,\underline{H}_e(\underline{M})$$

$$\underline{I} = \underline{H}_e^{inc}. \tag{2-5}$$

Since $\underline{M}$ and $\underline{I}$ have, respectively, the dimensions Volt/meter (V/m) and Ampère/meter (A/m), $\underline{Y}$ is an operator with the dimension of an admittance.

Define $\underline{G} = (\underline{Y} + \underline{Y}^*)/2$ and $\underline{B} = (\underline{Y} - \underline{Y}^*)/(2j)$, then

$$\underline{Y}(\underline{M}) = \underline{G}(\underline{M}) + j\underline{B}(\underline{M}). \tag{2-6}$$

In (2-6), $\underline{G}$ is a conductance operator and $\underline{B}$ is a susceptance operator. Following Harrington and Mautz [2], the

characteristic currents of the slot are defined to be the eigenfunctions $\underline{M}_n$ of the eigenvalue equation

$$\underline{Y}(\underline{M}_n) = y_n \, \underline{G}(\underline{M}_n) \tag{2-7}$$

so normalized that

$$\langle \underline{M}_n, \, \underline{G}(\underline{M}_n) \rangle = 1. \tag{2-8}$$

In (2-8), $\langle \cdot, \cdot \rangle$ denotes the inner product

$$\langle \underline{C}, \, \underline{D} \rangle = \int_{-w}^{+w} \underline{C}^{*}(x) \cdot \underline{D}(x) \, dx \tag{2-9}$$

where $\underline{C}^{*}(x)$ is the complex conjugate of $\underline{C}(x)$ and $\pm w$ are the x coordinates of the edges of the slot. Put

$$y_n = 1 + jb_n. \tag{2-10}$$

Then, using (2-6) and (2-10), (2-7) becomes

$$\underline{B}(\underline{M}_n) = b_n \, \underline{G}(\underline{M}_n). \tag{2-11}$$

The operators $\underline{G}$ and $\underline{B}$ are self-adjoint, since for any $\underline{M}_1$ and $\underline{M}_2$

$$\begin{aligned} \langle \underline{M}_1, \, \underline{G}(\underline{M}_2) \rangle &= \langle \underline{M}_1, \, \tfrac{1}{2}(\underline{Y} + \underline{Y}^{*})(\underline{M}_2) \rangle \\ &= \langle \tfrac{1}{2}(\underline{Y} + \underline{Y}^{*})(\underline{M}_1), \, \underline{M}_2 \rangle \\ &= \langle \underline{G}(\underline{M}_1), \, \underline{M}_2 \rangle \end{aligned} \tag{2-12}$$

and similarly for $\underline{B}$. Furthermore, $\underline{G}$ is positive definite, since the time-average power (per unit length in the y direction) radiated into the $z>0$ half-space

$$P_{rad} = \tfrac{1}{2}\,\mathrm{Re}\left[\int_{-w}^{+w} \underline{E} \times \underline{H}^{*}\Big|_{z=0} \cdot \underline{u}_z \, dx\right]$$

$$= \tfrac{1}{2}\,\mathrm{Re}\left[\int_{-w}^{+w} \underline{M} \cdot \underline{H}^{*} \, dx\right]$$

$$= \tfrac{1}{2}\,\mathrm{Re}\left[\tfrac{1}{2}\,\langle \underline{Y}(\underline{M}),\ \underline{M}\rangle\right]$$

$$= \tfrac{1}{4}\,\langle \underline{G}(\underline{M}),\ \underline{M}\rangle \qquad (2\text{-}13)$$

is always positive. The second and the last equalities in (2-13) follow from (2-1) and (2-12) respectively. It is then a standard practice [18, Section 1-25] to prove that all b_n, and hence $\underline{M}_n$, are real, and that $\underline{M}_n$ can be chosen to satisfy the orthogonality relationships

$$1.\ \langle \underline{M}_m,\ \underline{G}(\underline{M}_n)\rangle = \delta_{nm}$$

$$2.\ \langle \underline{M}_m,\ \underline{B}(\underline{M}_n)\rangle = b_n\,\delta_{nm} \qquad (2\text{-}14)$$

$$3.\ \langle \underline{M}_m,\ \underline{Y}(\underline{M}_n)\rangle = (1 + jb_n)\,\delta_{nm}$$

where δ_{nm} is the Kronecker delta function (0 if $m \neq n$, and 1 if $m=n$).

All the currents on a slot in a conducting plane in an unbounded medium are required to radiate some power however small. As can be seen from (2-11) and (2-13), the characteristic currents corresponding to very large b_n are basically non-radiating. It is shown in later chapters that, when the slot is very narrow, all the characteristic currents have very large eigenvalues $\{b_n\}$ and, therefore, are essentially non-radiating. In any case, all currents are required to exhibit the edge property ($M_x = O(\sqrt{w^2 - x^2})$ and $M_y = O(1/\sqrt{w^2 - x^2})$, as $x \to \pm w$) [19, Section 1-4].

2-3 Modal Solution of the Operator Equation

A modal solution of (2-4) for the magnetic current $\underline{M}$ over the slot is obtained in this section. Put

$$\underline{M} = \sum_n V_n \underline{M}_n \tag{2-15}$$

where $\underline{M}_n$ are the characteristic currents of the slot, and V_n are complex coefficients to be determined. Substituting (2-15) into (2-4), it then becomes

$$\sum_n V_n \underline{Y}(\underline{M}_n) = \underline{I}. \tag{2-16}$$

Taking the inner product of (2-16) with each $\underline{M}_m$, there results

$$\sum_n V_n \langle \underline{M}_m, \underline{Y}(\underline{M}_n) \rangle = \langle \underline{M}_m, \underline{I} \rangle. \tag{2-17}$$

Because of the third orthogonality relationship of (2-14), only the mth term in the summation survives. Thus

$$V_m \langle \underline{M}_m, \underline{Y}(\underline{M}_m) \rangle = \langle \underline{M}_m, \underline{I} \rangle. \tag{2-18}$$

Hence

$$V_m = \frac{\langle \underline{M}_m, \underline{I} \rangle}{1 + jb_m}. \tag{2-19}$$

Substituting (2-19) into (2-15), it becomes

$$\underline{M} = \sum_n \frac{\langle \underline{M}_n, \underline{I} \rangle}{1 + jb_n} \underline{M}_n. \tag{2-20}$$

The magnetic current $\underline{M}$ given by (2-20) is called the modal solution of (2-4).

2-4 Power Consideration

The total complex power entering the slot is basically

$$P_{in} = \tfrac{1}{2} \int_{-w}^{+w} \underline{E} \times \underline{H}^* \Big|_{z=0_-} \cdot \underline{u}_x \, dx. \tag{2-21}$$

Using (2-1), (2-4), and (2-5), (2-21) becomes

$$P_{in} = \tfrac{1}{2} \left(\langle \underline{I}, \underline{M} \rangle - \tfrac{1}{2} \langle \underline{Y}(\underline{M}), \underline{M} \rangle \right)$$

$$= \tfrac{1}{4} \langle \underline{I}, \underline{M} \rangle$$

$$= \tfrac{1}{4} \langle \underline{Y}(\underline{M}), \underline{M} \rangle. \qquad (2\text{-}22)$$

Furthermore, using (2-20), (2-22) becomes

$$P_{in} = \tfrac{1}{4} \left[\sum_n \frac{1 - jb_n}{1 + b_n^2} |\langle \underline{I}, \underline{M}_n \rangle|^2 \right]. \qquad (2\text{-}23)$$

Since the time-average power (2-13) radiated into the $z>0$ half-space is equal to the time-average power entering the slot, $\frac{1}{4}\langle \underline{G}(\underline{M}), \underline{M} \rangle$ is equal to the real part of the right-hand side of (2-23).

A parameter sometimes used to express the transmission characteristics of the slot is the transmission coefficient T. By definition, the transmission coefficient of the slot is the ratio of the time-average power transmitted through the slot to that incident on the slot [9, Section 7-12]. Using (2-23), T is readily found as

$$T = \frac{1}{4P} \sum_n \frac{1}{1 + b_n^2} |\langle \underline{I}, \underline{M}_n \rangle|^2 \qquad (2\text{-}24)$$

where P is the time-average power incident on the slot.

2-5 The Characteristic Fields of the Slot

The fields $(\underline{E}_n, \underline{H}_n)$ produced by the characteristic currents $\underline{M}_n$ are called the characteristic fields of the

slot. Orthogonality relationships for the characteristic fields over the radiation cylinder can be obtained from those for the characteristic currents by means of the complex Poynting theorem [9, Section 1-10]. These relationships are dual to those for the characteristic fields of the conducting body, and can be derived in a similar manner [20]. Thus

$$1.\ \frac{1}{\eta}\int_{C_{y\infty}} \underline{E}_m^* \cdot \underline{E}_n \, d\tau = \delta_{nm}$$

$$2.\ \eta\int_{C_{y\infty}} \underline{H}_m^* \cdot \underline{H}_n \, d\tau = \delta_{nm} \qquad (2\text{-}25)$$

$$3.\ \omega\int_{V} (\mu \underline{H}_m^* \cdot \underline{H}_n - \varepsilon \underline{E}_m^* \cdot \underline{E}_n) \, dv = -b_n \, \delta_{nm}$$

in duality with the orthogonality relationships for the conducting body. In (2-25), η is the wave impedance of the medium, $C_{y\infty}$ is the radiation cylinder, and the integration in (2-25.3) is over the whole space. Figure 2-2 shows the integration domain for (2-25).

The third orthogonality relationship of (2-25) states that the difference between the magnetic and electric energy stored in any characteristic field is $-b_n/(2\omega)$ Joules for every one Watt of radiated power. The characteristic fields

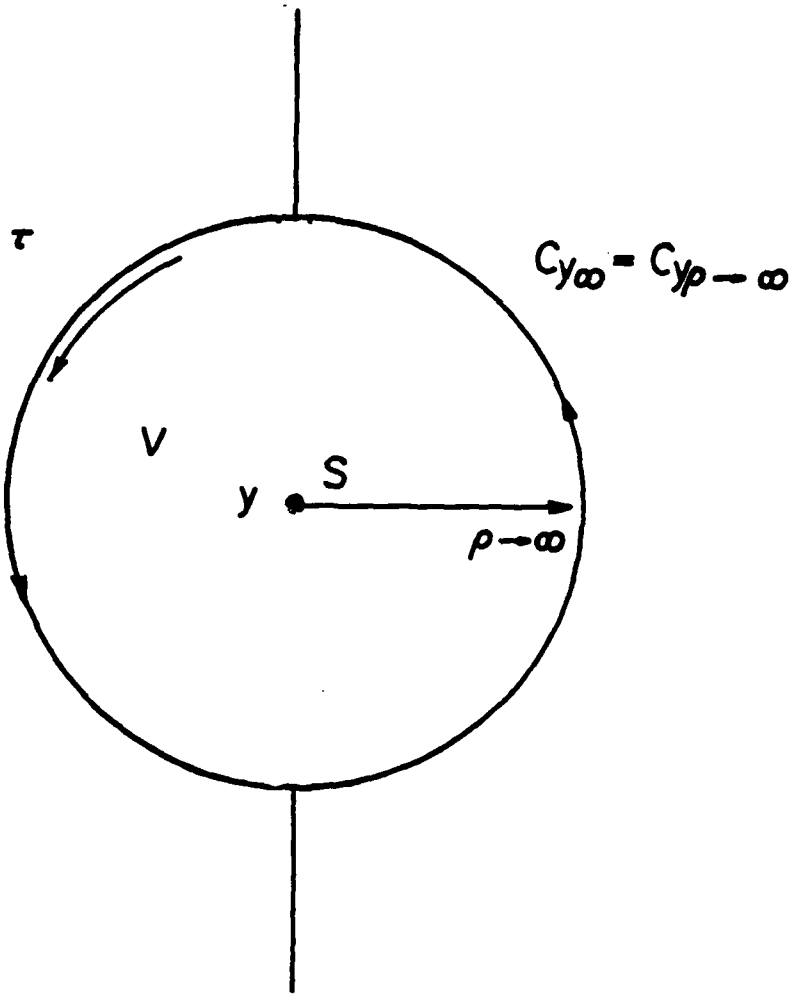

Figure 2-2. The integration domain of (2-25).

corresponding to positive (negative) b have predominantly stored electric (magnetic) energy, and are therefore referred to as the capacitive (inductive) modes of the slot. The characteristic fields corresponding to b=0 are then called the resonant modes of the slot.

A modal expansion of the field radiated by $\underline{M}$ in terms of the characteristic fields $\underline{E}_n$ and $\underline{H}_n$ can be readily obtained using the modal expansion (2-15) of $\underline{M}$:

$$\underline{E}(\underline{M}) = \sum_n V_n \underline{E}(\underline{M}_n) = \sum_n V_n \underline{E}_n$$

$$\underline{H}(\underline{M}) = \sum_n V_n \underline{H}(\underline{M}_n) = \sum_n V_n \underline{H}_n. \qquad (2\text{-}26)$$

In Appendix A, it is shown that the field $(\underline{E}(\underline{M}), \underline{H}(\underline{M}))$ given by (2-26) converges in a least-squares sense on the radiation cylinder.

2-6 Solution of the Eigenvalue Equation

An exact solution of the eigenvalue equation (2-11) for the characteristic currents is rather difficult, if at all possible. An approximate solution has then to be sought.

Put

$$S = \bigcup_{k=1}^{N} S_k \tag{2-27}$$

$$\underline{M}_n = \sum_{k=1}^{L} U_{nk}\, \underline{f}_k. \tag{2-28}$$

In (2-27), S_k are non-overlapping intervals such that

$$2w = \sum_{k=1}^{N} |S_k| \tag{2-29}$$

where $|S_k|$ is the length of the kth interval (see Figure 2-3). In (2-28), each $\underline{f}_k$ is a real function that is defined on a part of the partition and vanishes on the remainder of it, and U_{nk} are real coefficients to be determined. Substituting (2-28) into (2-11), it becomes

$$\sum_{k=1}^{L} U_{nk}\, \underline{B}(\underline{f}_k) = b_n \sum_{k=1}^{L} U_{nk}\, \underline{G}(\underline{f}_k) + \underline{R} \tag{2-30}$$

where $\underline{R}$ is a residual term.

A Galerkin solution [11, Section 1-3] of (2-11) can be obtained by requiring that $\underline{R}$ be orthogonal to all $\underline{f}_k$, viz.,

$$\langle \underline{f}_l, \underline{R} \rangle = 0 \qquad l=1,2,\ldots,L. \tag{2-31}$$

Thus, taking the inner product of (2-30) with each $\underline{f}_l$, and enforcing the Galerkin condition (2-31), there then results

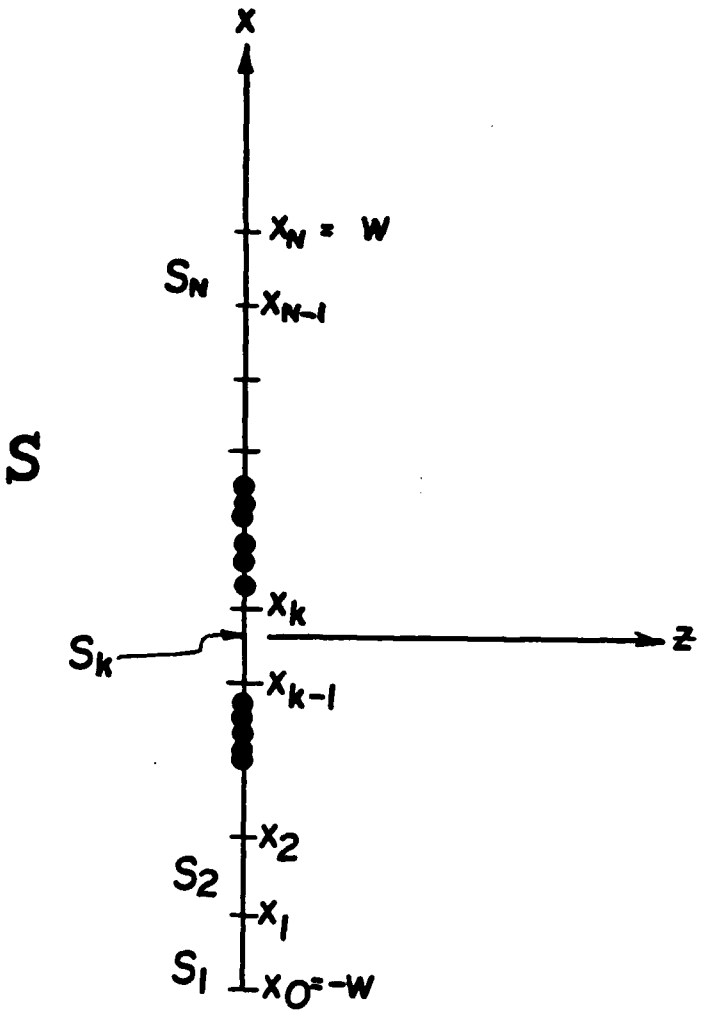

Figure 2-3. The partition of the slot.

$$\sum_{k=1}^{L} U_{nk} \langle \underline{f}_i, \underline{\underline{B}}(\underline{f}_k) \rangle = b_n \sum_{k=1}^{L} U_{nk} \langle \underline{f}_i, \underline{\underline{G}}(\underline{f}_k) \rangle$$

$$i=1,2,\ldots,L. \qquad (2\text{-}32)$$

In matrix form, (2-32) becomes

$$\underline{\underline{B}} \vec{U}_n = b_n \underline{\underline{G}} \vec{U}_n \qquad (2\text{-}33)$$

where $\underline{\underline{G}}$ and $\underline{\underline{B}}$ are the L by L matrices

$$\underline{\underline{G}} = [G_{ik}] = [\langle \underline{f}_i, \underline{\underline{G}}(\underline{f}_k) \rangle]$$

$$\underline{\underline{B}} = [B_{ik}] = [\langle \underline{f}_i, \underline{\underline{B}}(\underline{f}_k) \rangle] \qquad (2\text{-}34)$$

and $\vec{U}_n$ is the L by 1 vector

$$\vec{U}_n = [U_{nk}]. \qquad (2\text{-}35)$$

The constraint equation (2-8) now becomes

$$\vec{U}_n^T \underline{\underline{G}} \vec{U}_n = 1 \qquad (2\text{-}36)$$

where the superscript T denotes vector transpose.

The solution of (2-33) determines in a Galerkin sense the first L characteristic currents of the slot.

CHAPTER 3

TRANSVERSE ELECTRIC (TE) CASE

In this chapter, the characteristic currents and magnetic fields, the equivalent magnetic current, and the radiation pattern are computed for a general slot of arbitrary width in a conducting plane when it is illuminated by a uniform transverse electric (to the slot axis) plane wave. Analytic expressions for the narrow slot are also given.

3-1 Basic Formulation

Let a plane wave be incident on the slot at an angle θ from the left of the screen (see Figure 3-1). This wave is assumed uniform and transverse electric to the y-axis, and therefore has the field distribution

$$\underline{E}^i = \eta[\cos\theta\, \underline{u}_x - \sin\theta\, \underline{u}_z]\, e^{-jk(x\sin\theta + z\cos\theta)} \tag{3-1}$$

$$\underline{H}^i = e^{-jk(x\sin\theta + z\cos\theta)}\, \underline{u}_y .$$

Since the slot is uniform along the y-axis, and since the incident magnetic field has only an H_y component that does not vary with y, so does the scattered magnetic field.

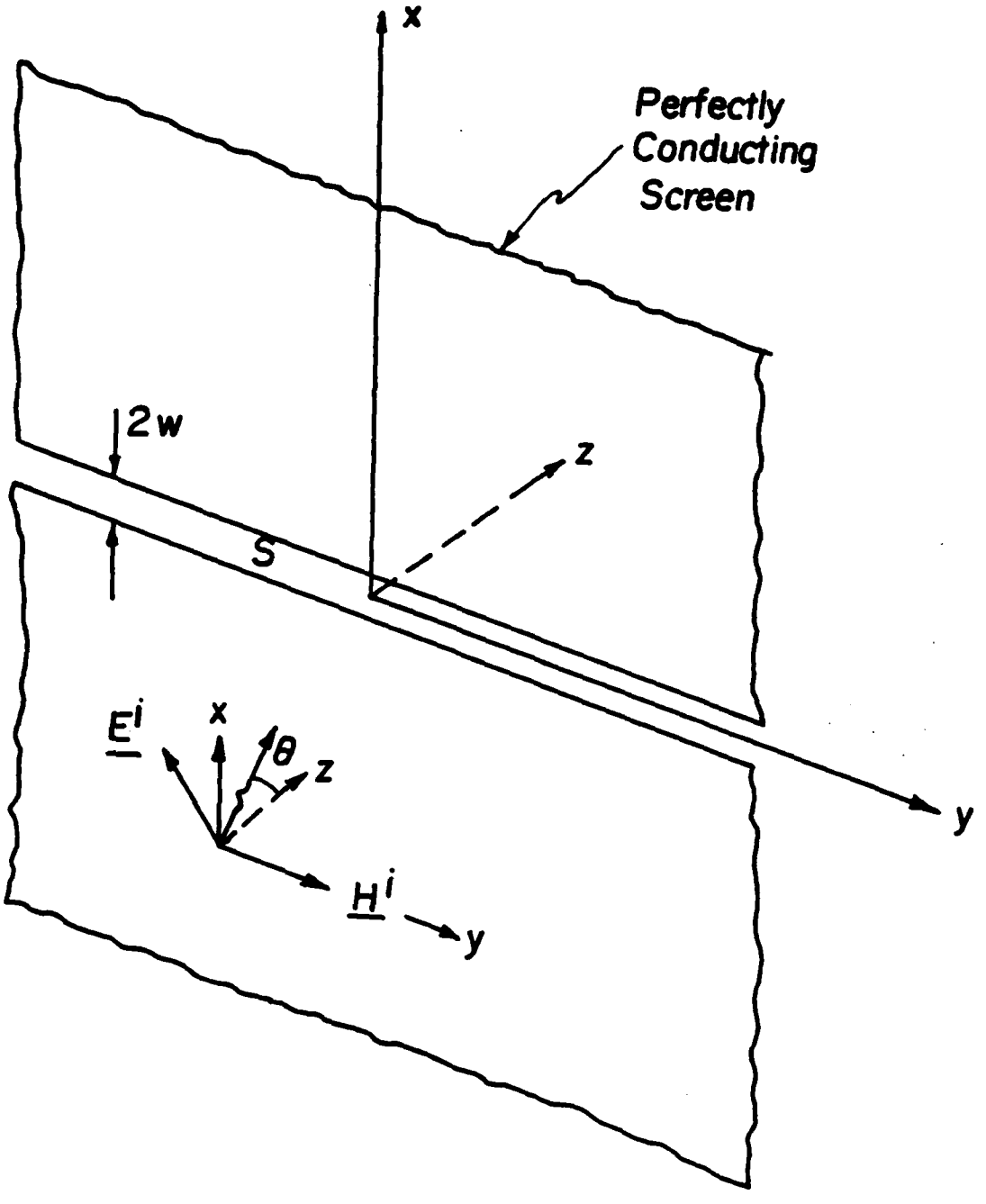

Figure 3-1. An infinitely long slot in a conducting plane illuminated by a uniform TE to the slot plane wave.

Consequently, the total field is independent of y and transverse electric to the y-axis. It then follows from (2-1) that $\underline{M}$ has only a y-component that does not vary with y:

$$\underline{M} = M(x)\ \underline{u}_y. \tag{3-2}$$

The field to the left of the screen is thus given by [9, Section 3-12]

$$\underline{E}(\underline{M}) = -\nabla \times \underline{F}(\underline{M})$$

$$\underline{H}(\underline{M}) = -j\frac{k}{\eta}\,\underline{F}(\underline{M}) \tag{3-3}$$

plus the short-circuit field

$$\underline{E}^{sc} = -2\eta[j\cos\theta \sin(kz\cos\theta)\ \underline{u}_x + \sin\theta \cos(kz\cos\theta)\ \underline{u}_z]\ e^{-jkx\sin\theta} \tag{3-4}$$

$$\underline{H}^{sc} = 2\cos(kz\cos\theta)\ e^{-jkx\sin\theta}\ \underline{u}_y.$$

In (3-3), $\underline{F}(\underline{M})$ is the electric vector potential produced by $\underline{M}$ in the presence of the complete screen, viz., [9, Section 5-7]:

$$\underline{F}(\underline{M}) = \frac{1}{2j}\int_{-w}^{+w} M(x')\ H_0^{(2)}\left(k\sqrt{z^2 + (x-x')^2}\right) dx'\ \underline{u}_y \tag{3-5}$$

where $H_o^{(2)}$ is the Hankel function of the second kind and zero order. The field to the right of the screen is then the negative of that in (3-3).

Substituting (3-3), (3-4), and (3-5) into (2-5), $\underline{Y}(\underline{M})$ and $\underline{I}$ are readily found as

$$\underline{Y}(\underline{M}) = \frac{k}{\eta} \int_{-w}^{+w} M(x') H_o^{(2)}(k|x-x'|)\, dx'\, \underline{u}_y \tag{3-6}$$

$$\underline{I} = 2 e^{-jkx \sin\theta}\, \underline{u}_y.$$

Since [9, Appendix D]

$$H_o^{(2)}(s) = J_o(s) - jN_o(s) \tag{3-7}$$

where J_o and N_o are the Bessel functions of the first kind and zero order, and of the second kind and zero order, respectively, the operators G(M) and B(M) in (2-6) are given by

$$G(M) = \frac{k}{\eta} \int_{-w}^{+w} M(x') \, J_o(k|x-x'|) \, dx'$$

(3-8)

$$B(M) = -\frac{k}{\eta} \int_{-w}^{+w} M(x') \, N_o(k|x-x'|) \, dx'.$$

In the next section, the eigenvalue equation (2-11) is solved for the special case of the narrow slot. The numerical solution of (2-11) for the general slot is then considered.

3-2 The Narrow Slot

An important case that requires special consideration is that of the narrow slot ($2kw \ll 1$).

Since

$$k|x-x'| \leq 2kw \ll 1 \qquad (3-9)$$

the Bessel functions J_o and N_o can be replaced by their small argument approximations [9, Appendix D]:

$$J_o(k|x-x'|) \approx 1 - \frac{k^2}{4}(x-x')^2$$

$$N_o(k|x-x'|) \approx \frac{2}{\pi} \log\left[\frac{\gamma k}{2}|x-x'|\right] \qquad (3\text{-}10)$$

where "log" denotes the natural logarithm and $\gamma = 1.7810724$. G(M) and B(M) are then given by

$$G(M) \approx \frac{k}{\eta} \int_{-w}^{+w} M(x') \left[1 - \frac{k^2}{4}(x-x')^2\right] dx'$$

$$B(M) \approx -\frac{2k}{\pi\eta} \int_{-w}^{+w} M(x') \log\left[\frac{\gamma k}{2}|x-x'|\right] dx'. \qquad (3\text{-}11)$$

Furthermore, I does not vary appreciably over S, and can therefore be approximated by the first two terms of its Taylor expansion about x=0. That is,

$$I \approx 2 - 2jkx \sin\theta \qquad x \in S \qquad (3\text{-}12)$$

or, on using (3-4),

$$I \approx H_y^{sc}(0) + j\frac{k}{\eta} E_x^{sc}(0)\, x \qquad x \in S \qquad (3\text{-}13)$$

where (0) is written for the point (x,z)=(0,0).

The characteristic currents of the narrow slot can be determined by solving (2-33) with G(M) and B(M) given by (3-11). Since the slot is narrow, however, partitioning of it is not necessary. The lkth elements of $\bar{\bar{G}}$ and $\bar{\bar{B}}$ then become

$$G_{lk} = \frac{k}{\eta} \int_{-w}^{+w} f_l(x)\, dx \int_{-w}^{+w} f_k(x') \left[1 - \frac{k^2}{4}(x-x')^2\right] dx' \tag{3-14}$$

$$B_{lk} = -\frac{2k}{\pi\eta} \int_{-w}^{+w} f_l(x)\, dx \int_{-w}^{+w} f_k(x') \log\left[\frac{\gamma k}{2}|x-x'|\right] dx'.$$

An appropriate choice of f_k that satisfies the edge requirements on M_y, and is compatible with (3-13), is

$$f_k(x) = \frac{x^{k-1}}{\sqrt{w^2 - x^2}} \qquad k=1,2. \tag{3-15}$$

Substituting (3-15) into (3-14), and using the identities

$$\int_{-w}^{+w} \frac{1}{\sqrt{w^2 - x^2}}\, dx = \pi$$

$$\int_{-w}^{+w} \frac{x^{2n-1}}{\sqrt{w^2 - x^2}}\, dx = 0 \qquad (3\text{-}16)$$

$$n>0$$

$$\int_{-w}^{+w} \frac{x^{2n}}{\sqrt{w^2 - x^2}}\, dx = \frac{\pi\, w^{2n}}{2^{2n}} \frac{(2n)!}{(n!)^2}$$

and [10, Appendix]

$$\int_{-w}^{+w} \frac{T_n(x'/w)}{\sqrt{w^2 - x'^2}} \log\left[\frac{\gamma k}{2}|x-x'|\right] dx' = \begin{cases} \pi \log(\gamma k w/4) & \text{if } n=0 \\ -\frac{\pi}{n} T_n(x/w) & \text{if } n>0 \end{cases} \qquad (3\text{-}17)$$

where $T_n(x)$ is the Chebyshev polynomial of the first kind and nth order, (2-33) then becomes

$$\frac{\pi k}{\eta} \begin{bmatrix} -2\log(\gamma k w/4) & 0 \\ 0 & w^2 \end{bmatrix} \begin{bmatrix} U_{n1} \\ U_{n2} \end{bmatrix}$$

$$= b_n \frac{\pi^2 k}{\eta} \begin{bmatrix} 1 - (kw/2)^2 & 0 \\ 0 & (w^2/2)(kw/2)^2 \end{bmatrix} \begin{bmatrix} U_{n1} \\ U_{n2} \end{bmatrix}. \qquad (3\text{-}18)$$

$$n=1,2$$

By inspection, then,

$$b_1 = -\frac{1}{\pi}\frac{2}{1-(kw/2)^2}\log(\gamma kw/4) \approx -\frac{2}{\pi}\log(\gamma kw/4) \tag{3-19}$$

$$M_1 = \frac{C}{\sqrt{w^2 - x^2}}$$

and

$$b_2 = \frac{8}{\pi(kw)^2} \tag{3-20}$$

$$M_2 = \frac{Dx}{\sqrt{w^2 - x^2}}$$

are the solution-pairs for (3-18). In (3-19) and (3-20), C and D are constants to be determined according to (2-36). Hence

$$M_1 = \frac{\sqrt{\eta/k}}{\pi}\frac{1}{\sqrt{w^2 - x^2}} \tag{3-21}$$

$$M_2 = \frac{2\sqrt{2\eta/k}}{\pi k w^2}\frac{x}{\sqrt{w^2 - x^2}}. \tag{3-22}$$

Furthermore, it readily follows from (3-19) and (3-20) that the characteristic values of the narrow slot are very large positive numbers whose ratio satisfies

$$\frac{b_2}{b_1} = \frac{-4}{(kw)^2 \log(\gamma kw/4)} = \frac{-4}{[(kw)\log(\gamma kw/4)](kw)} \geq \frac{4}{kw} \qquad (3\text{-}23)$$

The equivalent magnetic current M of the narrow slot is now given by

$$M = \frac{\langle M_1, I\rangle}{1 + jb_1} M_1 + \frac{\langle M_2, I\rangle}{1 + jb_2} M_2$$

$$\approx \frac{\langle M_1, I\rangle}{1 + jb_1} M_1 - j\frac{\langle M_2, I\rangle}{b_2} M_2$$

$$\approx \frac{1}{2}\left[j\frac{\eta}{k}\frac{H_y^{sc}(0)}{\nu + \log(kw/4) + j\pi/2} + E_z^{sc}(0)x\right]\frac{1}{\sqrt{w^2 - x^2}}. \qquad (3\text{-}24)$$

In (3-24), $\nu = \log(\gamma)$ is Euler's constant. Higher order solutions can be obtained by retaining more terms in the small argument approximations of Bessel functions in (3-10) and using more expansion functions. Incidentally, the magnetic current (3-24) is identical with the solution given in [10].

3-3 Evaluation of the Matrices $\bar{\bar{G}}$ and $\bar{\bar{B}}$

The solution of the eigenvalue equation (2-11) for an arbitrary slot can be effected by transforming the integral eigenvalue equation into an algebraic one as is seen in Section 2-6. However, the evaluation of the matrices $\bar{\bar{G}}$ and $\bar{\bar{B}}$ constitutes a large portion of the work involved in the solution. An efficient evaluation of these matrices is therefore necessary for the success of the solution.

The lkth elements of $\bar{\bar{G}}$ and $\bar{\bar{B}}$ are given by

$$\frac{\eta}{k} G_{lk} = \int_{-w}^{+w} f_l(x)\, dx \int_{-w}^{+w} f_k(x')\, J_0(k|x-x'|)\, dx' \tag{3-25}$$

$$\frac{\eta}{k} B_{lk} = -\int_{-w}^{+w} f_l(x)\, dx \int_{-w}^{+w} f_k(x')\, N_0(k|x-x'|)\, dx'$$

where the real functions f_k are so far unspecified. A particularly simple choice for f_k is

$$f_k = \begin{cases} 1 & \text{on } S_k \\ 0 & \text{on } S_l\ ,\ l \neq k \end{cases} \tag{3-26}$$

which is a pulse expansion function (see Figure 3-2). Using (3-26), the lkth elements of $\bar{\bar{G}}$ and $\bar{\bar{B}}$ become

$$\frac{\eta}{k} G_{lk} = \int_{x_{l-1}}^{x_l} dx \int_{x_{k-1}}^{x_k} J_o(k|x-x'|)\, dx' \tag{3-27}$$

$$\frac{\eta}{k} B_{lk} = -\int_{x_{l-1}}^{x_l} dx \int_{x_{k-1}}^{x_k} N_o(k|x-x'|)\, dx'.$$

Put

$$G_{lk}(x) = \int_{x_{k-1}}^{x_k} J_o(k|x-x'|)\, dx' \qquad x \in S_l. \tag{3-28}$$

$$B_{lk}(x) = -\int_{x_{k-1}}^{x_k} N_o(k|x-x'|)\, dx'$$

Then, by the first mean value theorem for integration [21, Section 7-18], there exist points x_{Jo} and $x_{No} \in S_l$ such that

$$\frac{\eta}{k} G_{lk} = |S_l|\, G_{lk}(x_{Jo}) \tag{3-29}$$

$$\frac{\eta}{k} B_{lk} = |S_l|\, B_{lk}(x_{No}).$$

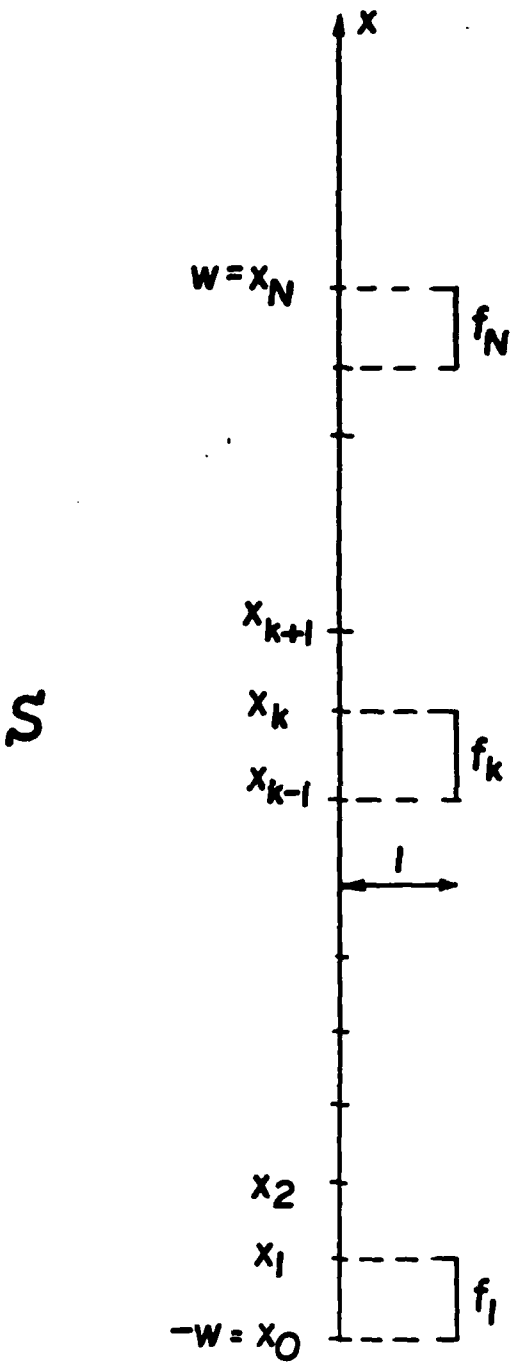

Figure 3-2. The pulse expansion functions for the characteristic currents.

The evaluation of G_{lk} and B_{lk} is completed by integrating the Bessel functions J_o and N_o over S_k, and, for that purpose, any quadrature rule can be used. Thus

$$\underset{k}{\eta}\, G_{lk} = \frac{1}{2}\,|S_l|\,|S_k| \sum_{i=1}^{Q} q_i\, J_o\left[k\,|x_{Jo} - x_i^k|\right] \tag{3-30}$$

$$\underset{k}{\eta}\, B_{lk} = -\frac{1}{2}\,|S_l|\,|S_k| \sum_{i=1}^{Q} q_i\, N_o\left[k\,|x_{No} - x_i^k|\right].$$

In (3-30), Q is the order of the rule, q_i are its coefficients, and its abscissas are given by

$$x_i^k = x_{k-1/2} + p_i \frac{|S_k|}{2} \tag{3-31}$$

where $x_{k-1/2}$ is the midpoint of S_k.

When evaluating the diagonal elements of $\bar{\bar{B}}$ $(l=k)$, N_o offers a logarithmic singularity at $x=x'$ that requires particular attention. Put

$$N_{op}(k\,|x-x'|) = (N_o - N_{os})(k\,|x-x'|) \tag{3-32}$$

where N_{os} is the singular part of N_o given by its small argument approximation (3-10). Then

$$\frac{\eta}{k} B_{ii} = -\int_{x_{i-1}}^{x_i} dx \int_{x_{i-1}}^{x_i} (N_{os} + N_{op})(k|x-x'|)\, dx'$$

$$= -\frac{1}{\pi} |S_i|^2 \left[2 \log\left[\gamma k \frac{|S_i|}{2}\right] - 3\right]$$

$$- \int_{x_{i-1}}^{x_i} dx \int_{x_{i-1}}^{x_i} N_{op}(k|x-x'|)\, dx'. \qquad (3\text{-}33)$$

N_{op} has no singularity at $x=x'$, and can therefore be integrated by the first mean value theorem and quadratures. Thus

$$\frac{\eta}{k} B_{ii} = -\frac{1}{\pi} |S_i|^2 \left[2 \log\left[\gamma k \frac{|S_i|}{2}\right] - 3\right]$$

$$- \frac{1}{2} |S_i|^2 \sum_{i=1}^{Q} q_i N_{op}\left[k|x_{NOp} - x_i^1|\right] \qquad (3\text{-}34)$$

for some $x_{NOp} \in S_i$.

Actually, finding such points x_{JO}, x_{NO}, and x_{NOp} is at least as difficult as computing the integrals themselves. For sufficiently small $|S_i|$, however, the midpoint of S_i can replace these points while introducing negligible error. Thus, dividing by the factor $|S_i|$,

$$\frac{\eta}{k|S_l|} G_{lk} = \frac{1}{2} |S_k| \sum_{i=1}^{Q} q_i J_0(u_i{}^{lk}) \qquad \text{for all } l,k$$

$$\frac{\eta}{k|S_l|} B_{lk} = \begin{cases} -\frac{1}{2} |S_k| \sum_{i=1}^{Q} q_i N_0(u_i{}^{lk}) & \text{if } l \neq k \\ -|S_l| \left[\frac{1}{\pi} \left[2 \log \left[\gamma k \frac{|S_l|}{2} \right] - 3 \right] + \frac{1}{2} \sum_{i=1}^{Q} q_i N_{0p}(u_i{}^{lk}) \right] & \text{if } l = k \end{cases} \tag{3-35}$$

where

$$u_i{}^{lk} = k|x_{l-1/2} - x_i{}^k|. \tag{3-36}$$

The matrices $\bar{\bar{G}}$ and $\bar{\bar{B}}$ so obtained are the same as those resulting from enforcing the point matching condition

$$R(x_{l-1/2}) = 0 \qquad l=1,2,\ldots,N \tag{3-37}$$

in (2-30), rather than the Galerkin condition (2-31), except for a slight alteration in B_{ll}, as can easily be established.

3-4 Numerical Results

The characteristic currents and magnetic fields as well as the equivalent magnetic current and radiation pattern have been computed for different slot widths. The computational aspects of the solution, and some of the results obtained for slots of width 0.4λ, 0.5λ, and 1.0λ where λ is the wavelength are discussed in this section.

In the actual computation, polynomial approximations of the Bessel functions J_0 and N_0 [22, Articles 9.4.1-9.4.3] are utilized, while all the integrals are computed using an eight-point Gaussian quadrature [22, Table 25.4]. In evaluating the far fields, the Hankel function is first replaced by its large argument approximation [9, Appendix D]:

$$H_0^{(2)}(s) = \sqrt{2j/(s\pi)}\; e^{-js}. \qquad (3\text{-}38)$$

Then, using the typical radiation zone approximations [9, Section 2-10],

$$s = k\sqrt{z^2 + (x-x')^2} = k(r - x'\cos\phi) \qquad (3\text{-}39)$$

$$1/s = 1/kr$$

for all points $(x,z)\in C_{yr}$, $r>>2w$, where ϕ is the angle $\mathbf{r}=x\mathbf{u}_x+z\mathbf{u}_z$ makes with the x-axis, the electric vector

potential produced by the characteristic current $\underline{M}_n$ at any point $(r,\emptyset)\in C_{yr}$ is readily found as

$$\underline{F}(\underline{M}_n) = \frac{\pm 1}{\sqrt{2j\pi kr}} e^{-jkr} \sum_{k=1}^{N} U_{nk} \int_{x_{k-1}}^{x_k} e^{jkx'\cos\emptyset}\, dx'\ \underline{u}_y$$

$$= \pm A(kr) \sum_{k=1}^{N} U_{nk} |S_k| e^{jkx_{k-1/2}\cos\emptyset} \cdot \frac{\sin((k|S_k|\cos\emptyset)/2)}{(k|S_k|\cos\emptyset)/2} \underline{u}_y \qquad (3\text{-}40)$$

where

$$A(kr) = \frac{e^{-jkr}}{\sqrt{2j\pi kr}}$$

and where the upper sign is used for $z<0$ and the lower one for $z>0$. The far characteristic fields then follow by substituting (3-40) into (3-3).

An IMSL Library 2 subroutine "EIGZF" [23] is used to solve the matrix eigenvalue equation (2-33) for the characteristic values and currents. In all the computer runs, a "performance index" has consistently been less than one, indicating that the subroutine has performed well. The convergence patterns for the characteristic values for the 0.4 λ , 0.5 λ , and 1.0 λ slots are shown in Tables 3-1, 3-2, and 3-3, respectively. As can be seen, the

Table 3-1

The convergence of the characteristic values for the 0.4 λ slot.

	N	b_1	b_2	b_3	b_4	b_5	...
	4	0.386499	2.541965	52.985104	7.204746×10^{3}	*	*
	8	0.382960	2.381441	39.523594	2.778433×10^{3}	4.624070×10^{5}	*
	12	0.381978	2.340359	37.074282	2.372682×10^{3}	3.329886×10^{5}	*
	16	0.381576	2.322112	36.091969	2.232416×10^{3}	2.945282×10^{5}	*
	20	0.381381	2.311973	35.573169	2.163472×10^{3}	2.775236×10^{5}	*
→	24	0.381277	2.305593	35.256428	2.123233×10^{3}	2.700021×10^{5}	*

Table 3-2

The convergence of the characteristic values for the 0.5λ slot.

N	b_1	b_2	b_3	b_4	b_5	...
4	0.248621	1.722857	22.177586	1.848905×10^{3}	*	*
8	0.251433	1.615827	16.842234	0.726753×10^{3}	0.767466×10^{5}	*
12	0.252425	1.588517	15.861717	0.622888×10^{3}	0.554707×10^{5}	*
16	0.252971	1.576381	15.466336	0.586800×10^{3}	0.494704×10^{5}	*
20	0.253329	1.569636	15.256797	0.569042×10^{3}	0.466199×10^{5}	*
→ 24	0.253587	1.565691	15.128519	0.558653×10^{3}	0.450576×10^{5}	*

Table 3-3

The convergence of the characteristic values for the 1.0λ slot.

N	b_1	b_2	b_3	b_4	b_5	b_6	b_7	...
4	-0.0592173	0.3201691	1.9221747	25.7259409	*	*	*	*
8	-0.0194068	0.3058703	1.6039377	12.3455109	0.2868804×10^{3}	1.4943577×10^{4}	17.0626604×10^{5}	∞
12	-0.0058205	0.3040117	1.5428879	10.9870705	0.2161946×10^{3}	0.8410060×10^{4}	5.5500121×10^{5}	∞
16	0.0009632	0.3034440	1.5176536	10.4968898	0.1953714×10^{3}	0.6970954×10^{4}	4.0148647×10^{5}	∞
20	0.0050257	0.3032162	1.5040598	10.2497418	0.1857875×10^{3}	0.6377427×10^{4}	3.4619262×10^{5}	∞
24	0.0077305	0.3031168	1.4956417	10.1026733	0.1803898×10^{3}	0.6061940×10^{4}	3.1878485×10^{5}	∞
28	0.0096609	0.3030754	1.4899555	10.0059495	0.1769714×10^{3}	0.5870056×10^{4}	3.0428758×10^{5}	∞
32	0.0111081	0.3030634	1.4858791	9.9379017	0.1746300×10^{3}	0.5742663×10^{4}	2.9314329×10^{5}	∞
36	0.0122334	0.3030671	1.4828270	9.8876526	0.1729390×10^{3}	0.5651750×10^{4}	2.8856119×10^{5}	∞
→40	0.0131335	0.3030794	1.4804643	9.8491539	0.1716661×10^{3}	0.5586517×10^{4}	2.8273049×10^{5}	∞

convergence is always monotone, either upward, or downward. For the 1.0 λ slot, b_2 first decreases monotonically and then increases, but this can be attributed to rounding errors. Also, the convergence of the lower order characteristic values is generally faster than that of the higher order ones.

Any calculated value of b_n is probably inaccurate whenever $|b_n/b_1| > 10^{NS}$ where NS is the number of significant figures retained during the calculation. Whenever b_n was large enough to be unreliable, it was arbitrarily set equal to ∞. Now, the contribution of these currents is extremely small, and therefore has not been considered in subsequent computations. It appears that for a slot in a conducting plane in an unbounded medium, only a finite number of characteristic currents need to be computed. This is also expected to carry over to slots in a conducting plane separating contrasting mediums.

The computed characteristic currents normalized to a maximum amplitude of unity and their radiation patterns for the slots considered are shown in Figures 3-3, 3-5, 3-7, 3-9, 3-11 and 3-13. Figures 3-5, 3-9, and 3-13 are polar plots. The normalization to a maximum amplitude of unity is used only for plotting convenience. The equivalent magnetic currents and radiation patterns for the slots are

shown in Figures 3-4, 3-6, 3-8, 3-10, 3-12, and 3-14. Figures 3-6, 3-10, and 3-14 are polar plots. All currents clearly exhibit the right behavior at the edges. It is interesting to note that the number of lobes in each pattern is equal to the order of the characteristic current or field. When a slot is excited by the plane wave (3-1) with $\theta=0^{\circ}$, the equivalent magnetic current $\underline{M}$ is given by (2-15). The power radiated by the magnetic current $V_n\underline{M}_n$ is called P_n. For various values of n, the ratio P_n/P_1 is given in Table 3-4. This ratio was evaluated with N as specified in the arrow marked rows in Tables 3-1, 3-2, and 3-3. The entries in Table 3-4 suggest that the radiation pattern for the slot is basically the same as that for its dominant characteristic current. This is indeed the case, as is readily established by comparing the corresponding figures.

Table 3-4

The ratio of the power radiated by each characteristic current to that radiated by the dominant characteristic current for a (a) 0.4λ slot, (b) 0.5λ slot, and (c) 1.0λ slot.

(a)

n	P_n / P_1
1	1.0
2	0.159567
3	5.170679×10^{-3}
4	6.807077×10^{-5}
5	5.374193×10^{-7}
...	0.0

(b)

n	P_n / P_1
1	1.0
2	0.267814
3	1.145190×10^{-2}
4	2.366575×10^{-4}
5	2.929748×10^{-6}
...	0.0

(c)

n	P_n / P_1
1	1.0
2	0.149602
3	0.039083
4	3.766960×10^{-3}
5	1.726436×10^{-4}
6	5.240201×10^{-6}
7	1.126339×10^{-7}
...	0.0

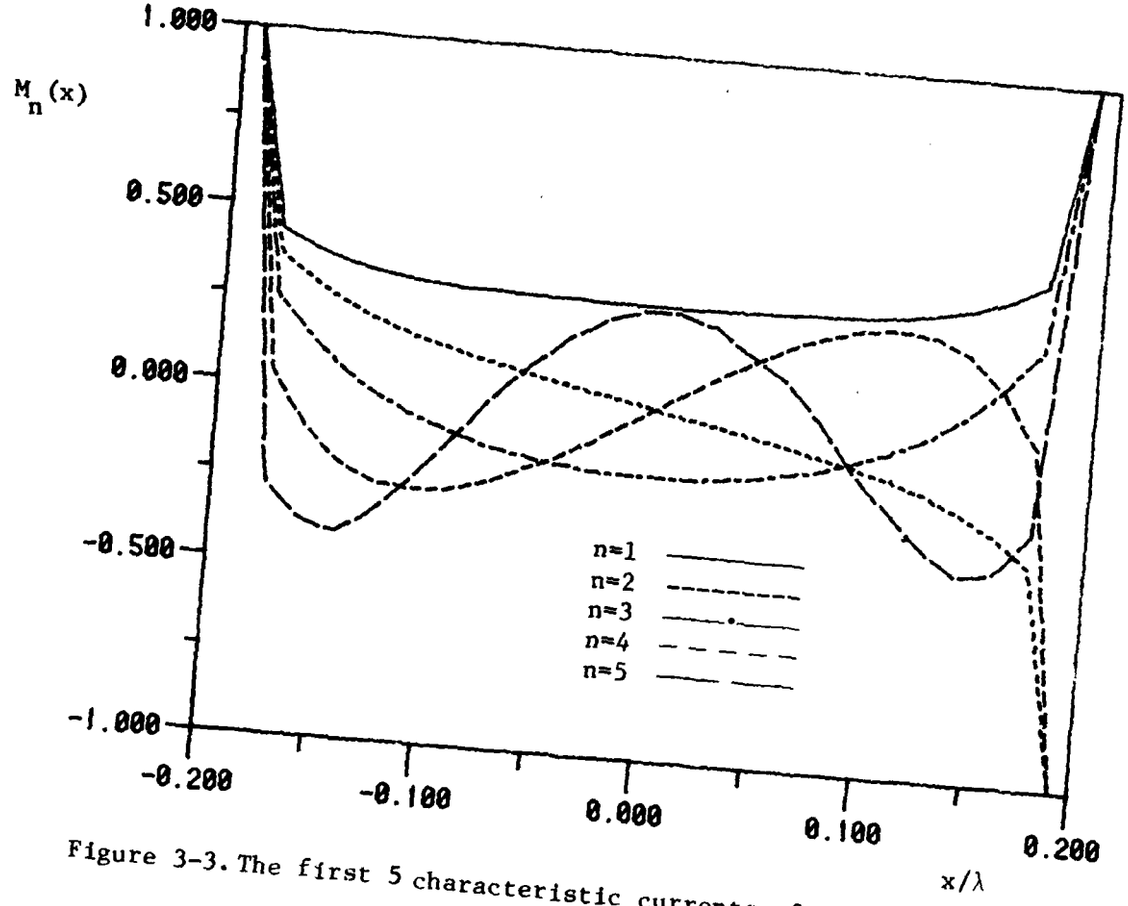

Figure 3-3. The first 5 characteristic currents for the 0.4λ slot.

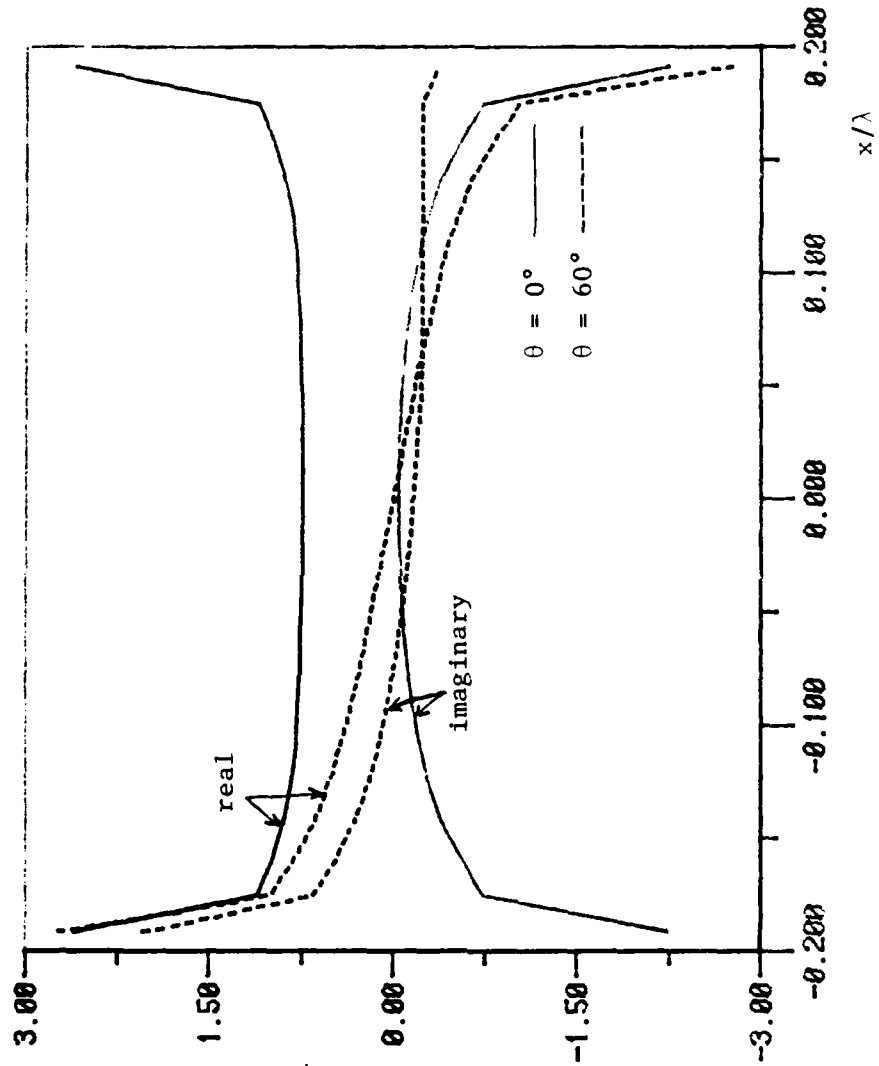

Figure 3-4. The equivalent magnetic current for the 0.4λ slot.

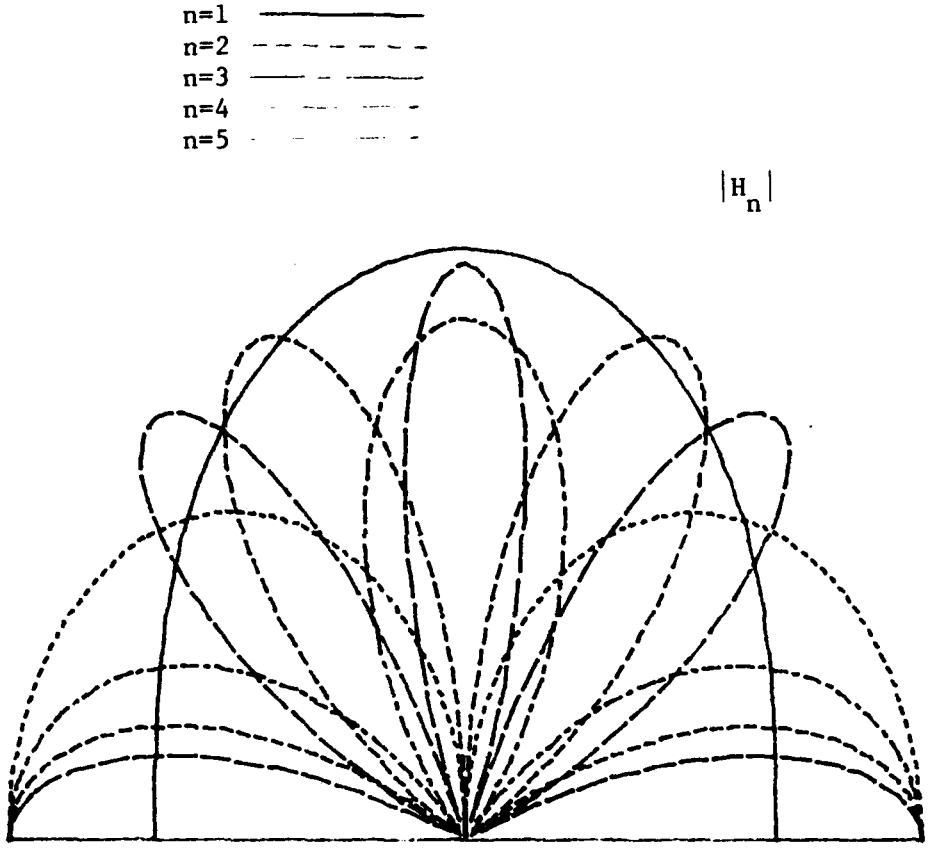

Figure 3-5. The radiation patterns for the first 5 characteristic magnetic fields for the 0.4λ slot.

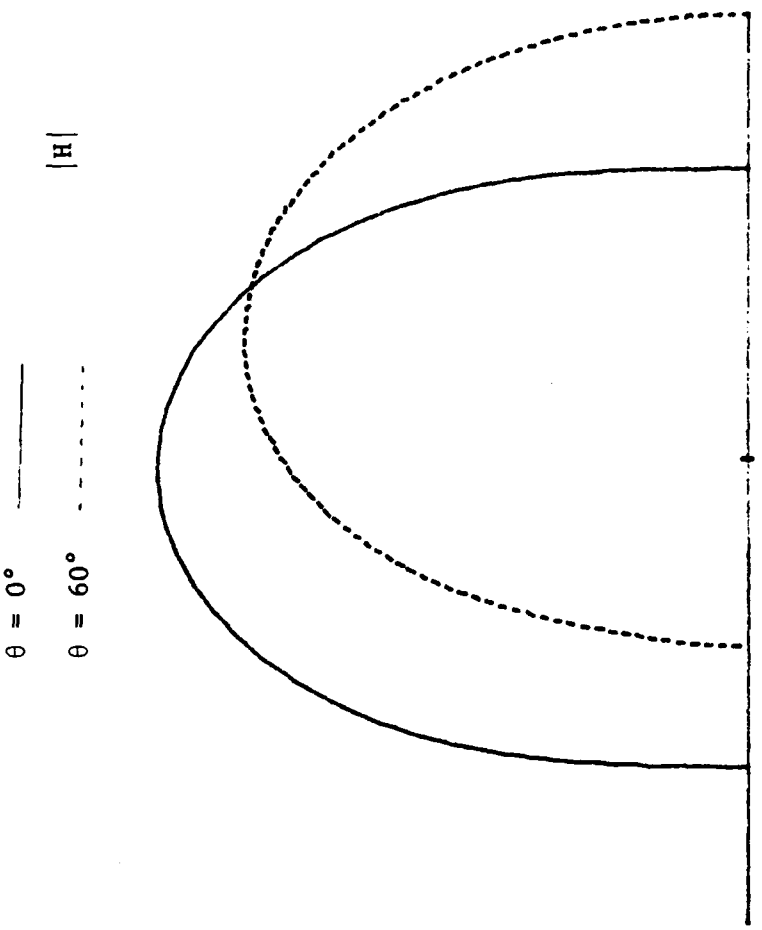

Figure 3-6. The radiation pattern for the 0.4λ slot.

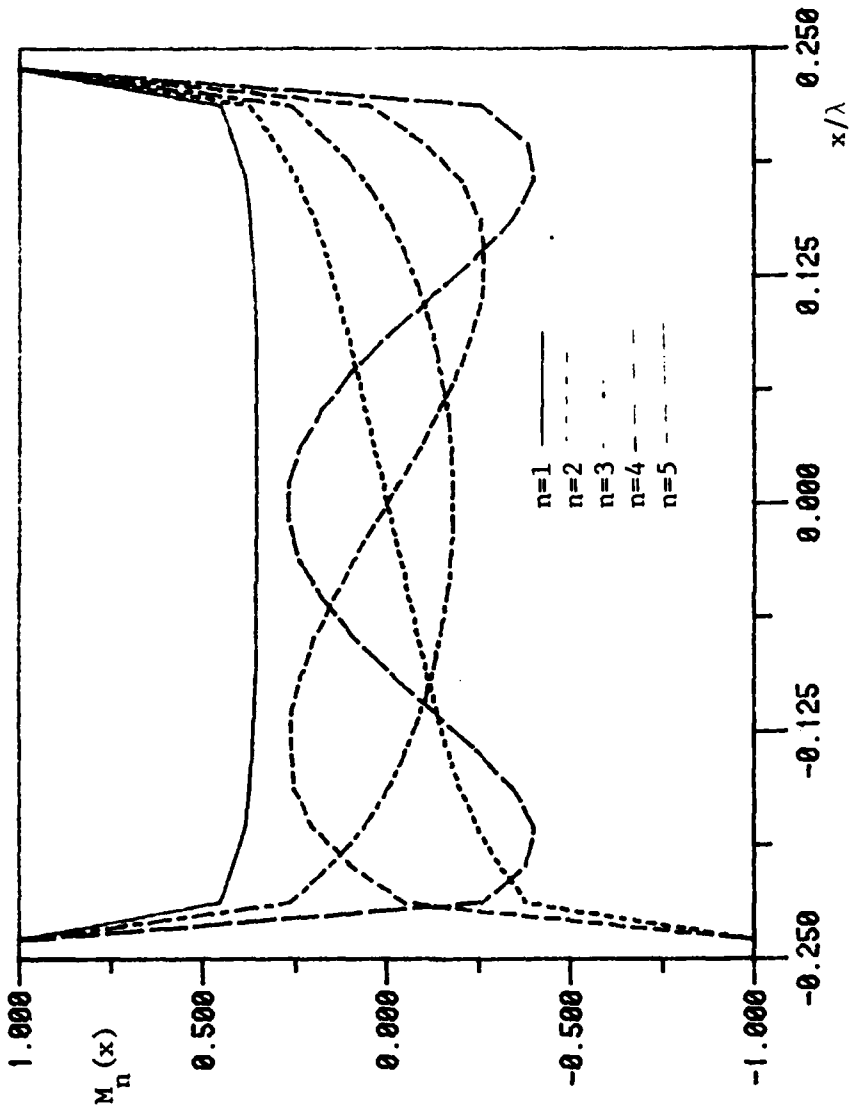

Figure 3-7. The first 5 characteristic currents for the 0.5λ slot.

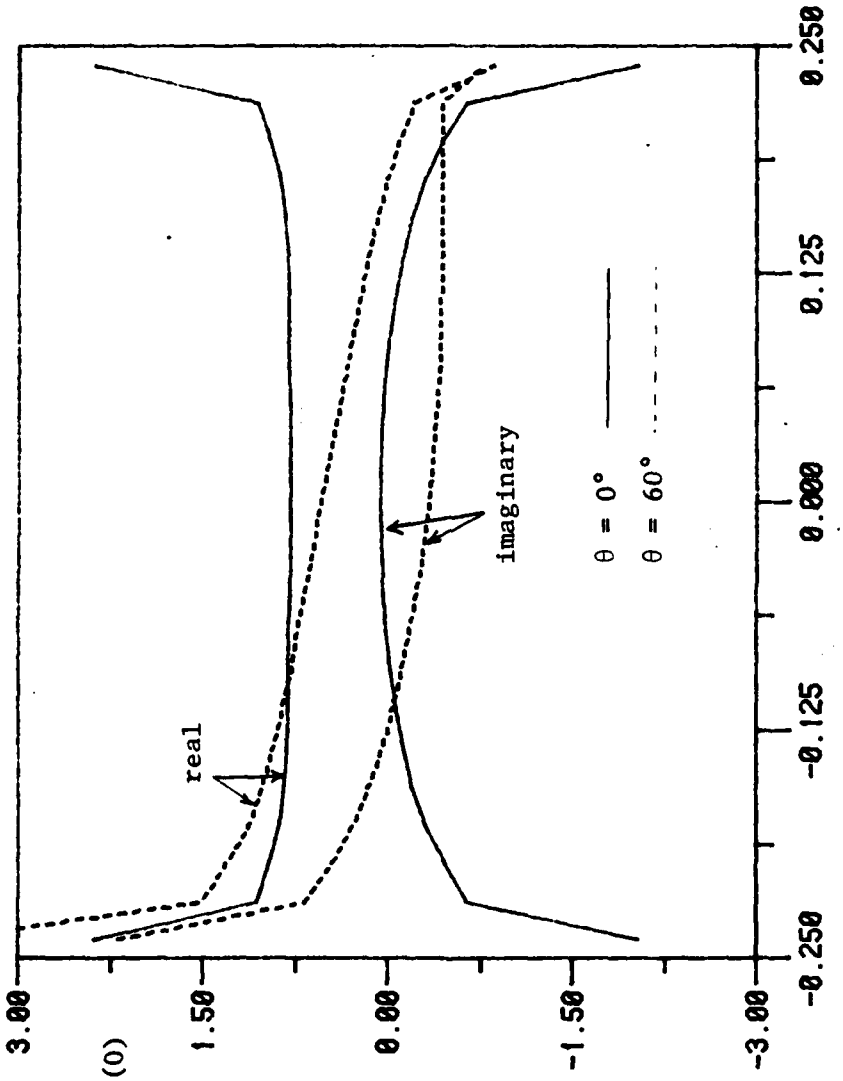

Figure 3-8. The equivalent magnetic current for the 0.5λ slot.

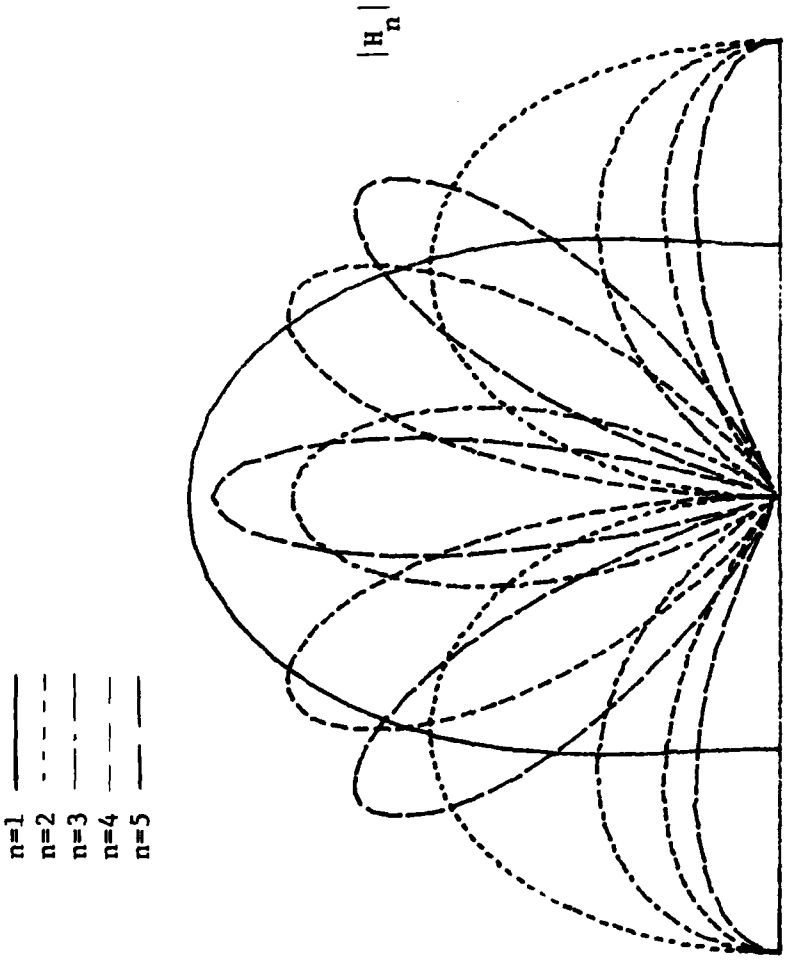

Figure 3-9. The radiation patterns for the first 5 characteristic magnetic fields for the 0.5λ slot.

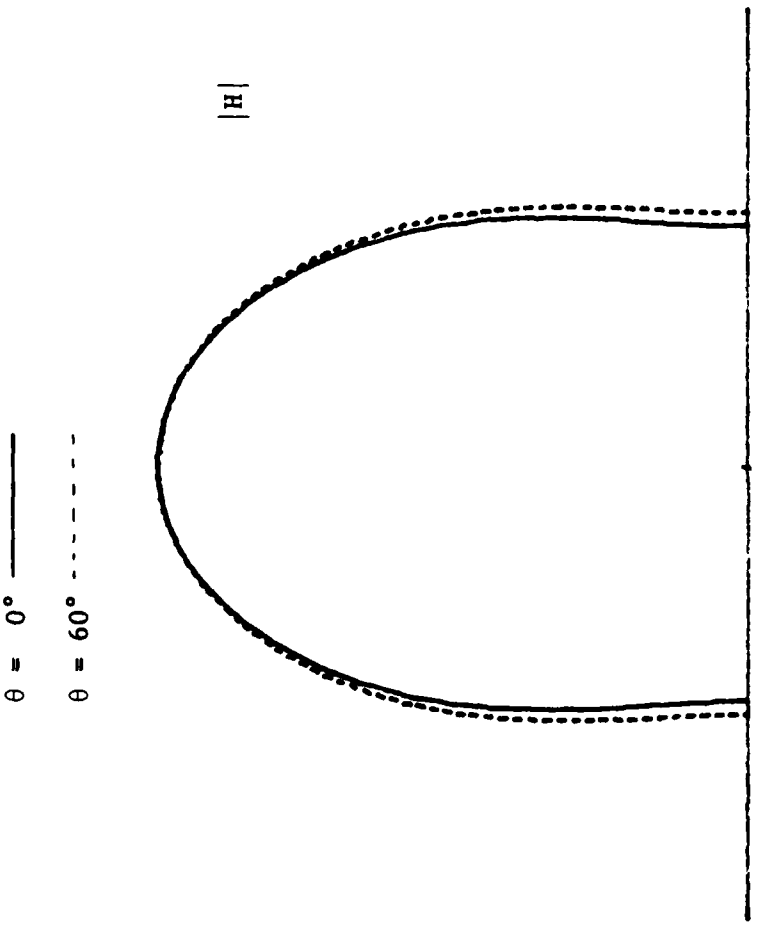

Figure 3.10. The radiation pattern for the 0.5λ slot.

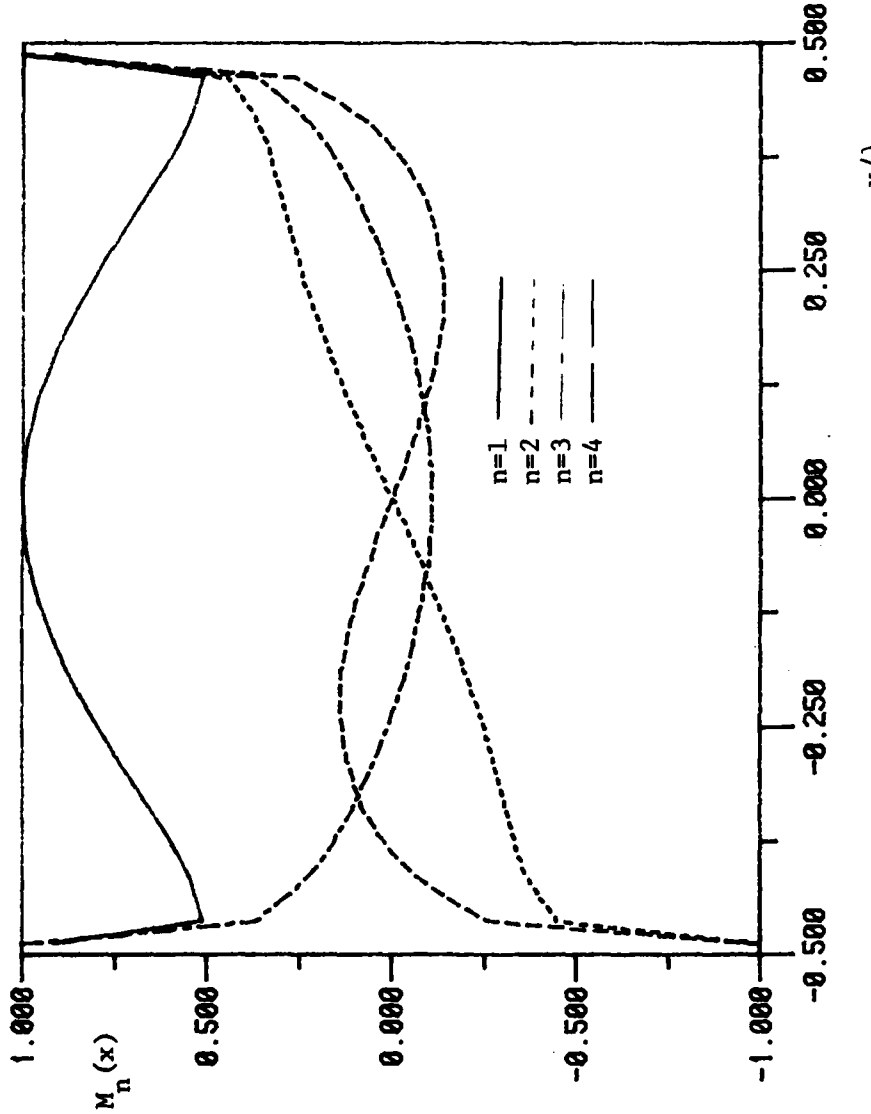

Figure 3-11(a). The first 4 characteristic currents for the 1.0λ slot.

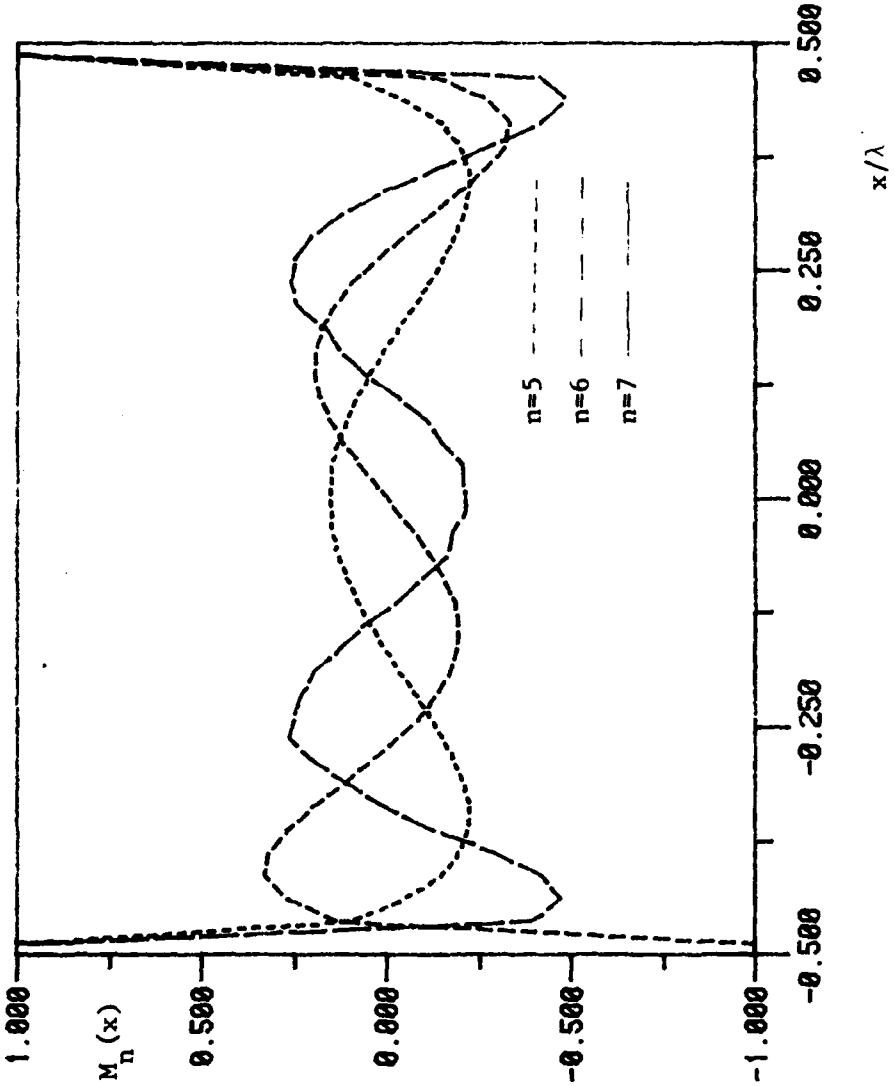

Figure 3-11(b). The 5th, 6th, and 7th characteristic currents for the 1.0λ slot.

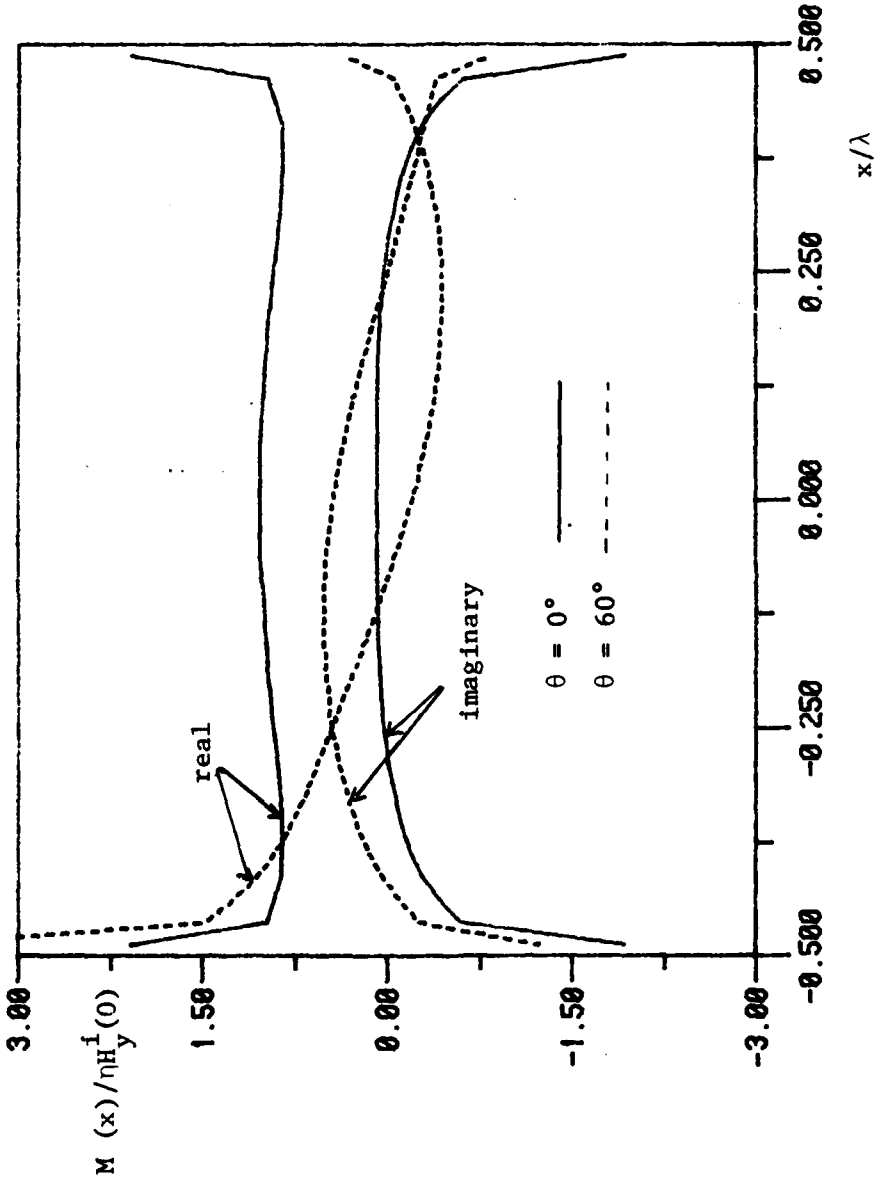

Figure 3-12. The equivalent magnetic current for the 1.0λ slot.

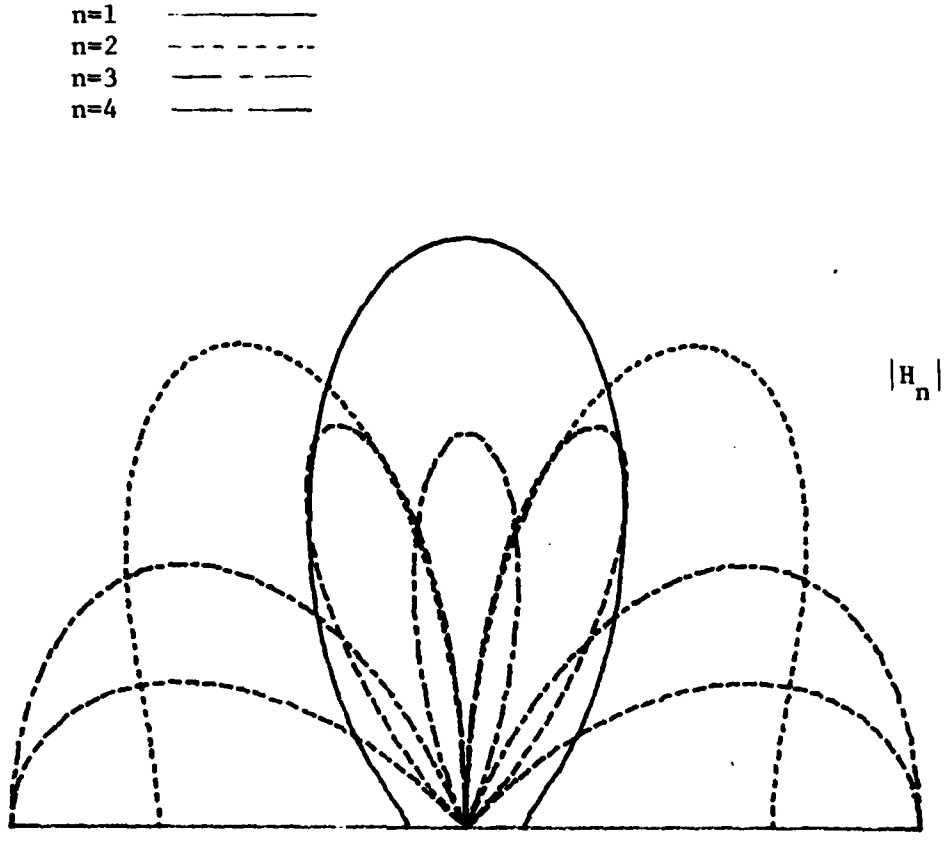

Figure 3-13(a) The radiation patterns for the first 4 characteristic magnetic fields for the 1.0λ slot.

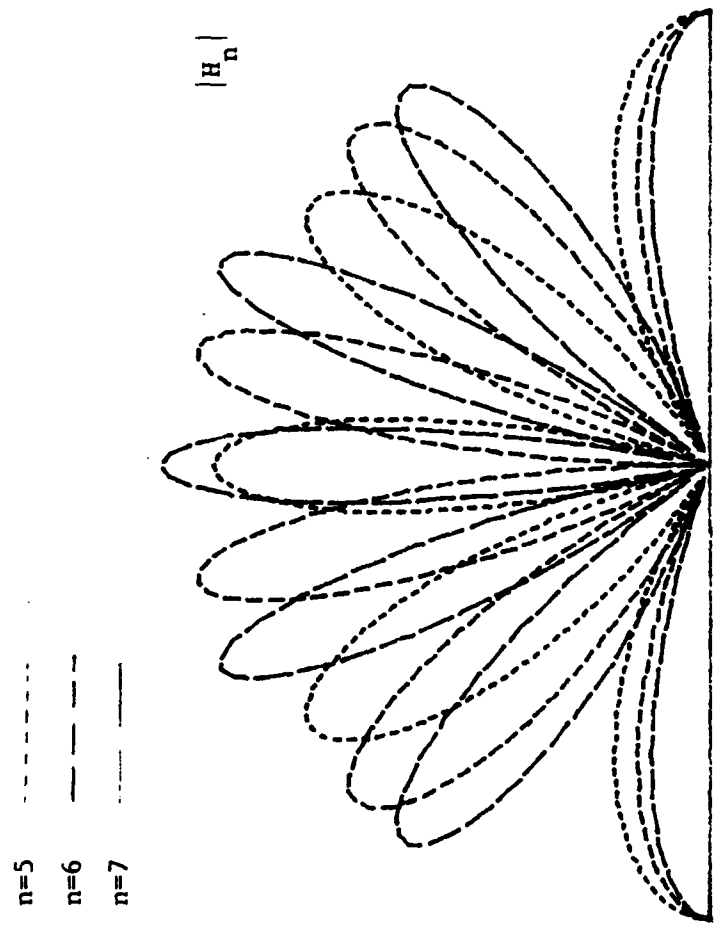

Figure 3-13(b) The radiation patterns for the 5th, 6th, and 7th characteristic magnetic fields for the 1.0λ slot.

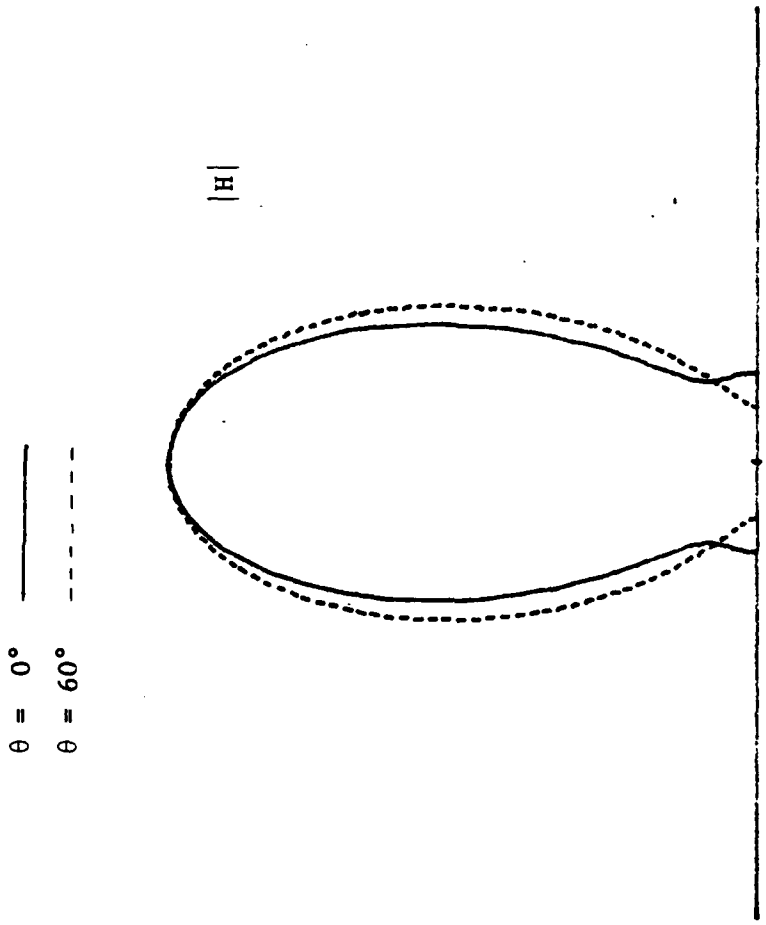

Figure 3-14. The radiation pattern for the 1.0λ slot.

CHAPTER 4

TRANSVERSE MAGNETIC (TM) CASE

The case of a uniform transverse magnetic (to the slot axis) plane wave excitation of the slot is considered in this chapter. The characteristic currents and electric fields as well as the equivalent magnetic current and radiation pattern are determined for different slots. Analytic expressions for the narrow slot are also given.

4-1 Basic Formulation

Let a plane wave be incident on the slot at an angle θ from the left of the screen (see Figure 4-1). This wave is assumed uniform and transverse magnetic to the y-axis, and therefore has the field distribution

$$\underline{E}^i = e^{-jk(x\sin\theta + z\cos\theta)}\,\underline{u}_y \tag{4-1}$$

$$\underline{H}^i = -\frac{1}{\eta}\left[\cos\theta\,\underline{u}_x - \sin\theta\,\underline{u}_z\right]e^{-jk(x\sin\theta + z\cos\theta)}.$$

Since the slot is uniform along the y-axis, and since the incident electric field has only an E_y component that does not vary with y, so does the scattered electric field. Consequently, the total field is independent of y and

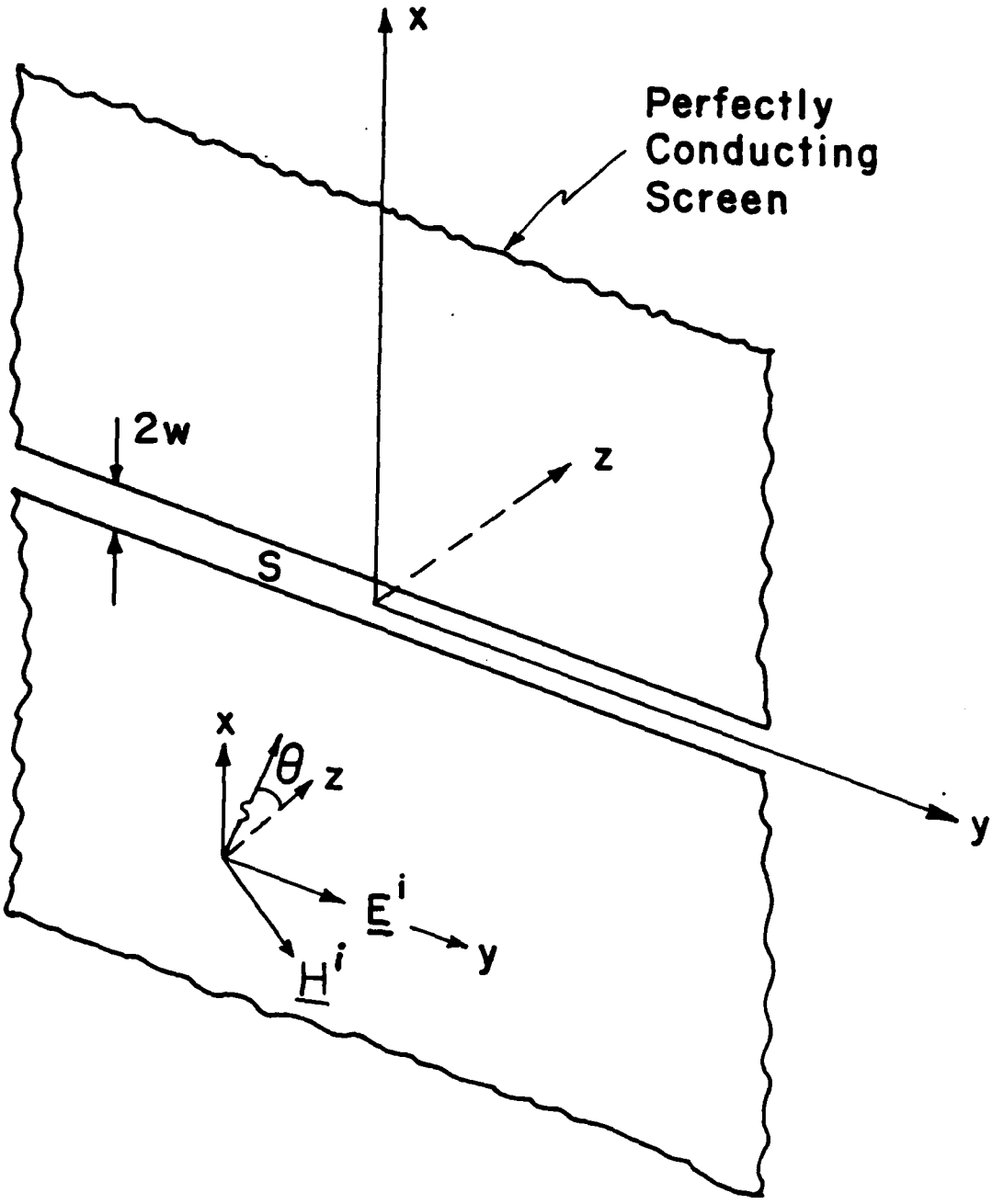

Figure 4-1. An infinitely long slot in a conducting plane illuminated by a uniform TM to the slot plane wave.

transverse magnetic to the y-axis. It then follows from (2-1) that $\underline{M}$ has only an x-component that does not vary with y:

$$\underline{M} = M(x)\ \underline{u}_x . \tag{4-2}$$

The field to the left of the screen is thus given by [9, Section 3-12]

$$\underline{E}(\underline{M}) = -\nabla \times \underline{F}(\underline{M})$$

$$\underline{H}(\underline{M}) = -j\frac{1}{\eta k}\left[\nabla(\nabla \cdot \underline{F}(\underline{M})) + k^2\,\underline{F}(\underline{M})\right] \tag{4-3}$$

plus the short circuit field

$$\underline{E}^{sc} = -j2\sin(kz\cos\theta)\, e^{-jkx\sin\theta}\,\underline{u}_y$$

$$\underline{H}^{sc} = -\frac{2}{\eta}\left[\cos\theta\cos(kz\cos\theta)\,\underline{u}_x + j\sin\theta\sin(kz\cos\theta)\,\underline{u}_z\right] e^{-jkx\sin\theta} . \tag{4-4}$$

In (4-3), $\underline{F}(\underline{M})$ is the electric vector potential produced by $\underline{M}$ in the presence of the complete screen, viz. [9, Section 5-7]:

$$\underline{F}(\underline{M}) = \frac{1}{2j}\int_{-w}^{+w} M(x')\, H_0^{(2)}\left(k\sqrt{z^2 + (x-x')^2}\right) dx'\ \underline{u}_x . \tag{4-5}$$

The field to the right of the screen is then the negative of that in (4-3).

Substituting (4-3), (4-4), and (4-5) into (2-5), Y(M) and I are readily found as

$$Y(M) = \frac{1}{k\eta}\left(\frac{d^2}{dx^2} + k^2\right)\int_{-w}^{+w} M(x')\, H_o^{(2)}(k|x-x'|)\, dx' \tag{4-6}$$

$$I = -\frac{2}{\eta}\cos\theta\, e^{-jkx\sin\theta}$$

where, as before, scalar quantities are used since $\underline{Y}(\underline{M})$ and $\underline{I}$ are both directed along the x-axis. Furthermore, using (3-7), the operators G(M) and B(M) are now given by

$$G(M) = \frac{1}{k\eta}\left(\frac{d^2}{dx^2} + k^2\right)\int_{-w}^{+w} M(x')\, J_o(k|x-x'|)\, dx' \tag{4-7}$$

$$B(M) = -\frac{1}{k\eta}\left(\frac{d^2}{dx^2} + k^2\right)\int_{-w}^{+w} M(x')\, N_o(k|x-x'|)\, dx'.$$

Below, the narrow slot is treated first, and is then followed by the general case of an arbitrary slot.

4-2 The Narrow Slot

Approximations similar to those utilized in the TE case can be used to simplify the analysis of a narrow slot excited by a uniform transverse magnetic plane wave. Specifically, the Bessel functions J_o and N_o are replaced by their small argument approximations (3-10). Furthermore, for a narrow slot, I does not vary greatly over the slot, and can therefore be approximated by the first two terms of its Taylor expansion about the origin, viz.:

$$I \approx H^{inc}(0) + x\, H^{inc\,\prime}(0)$$

$$= -\frac{1}{\eta}\left[2\cos\theta - jkx\,\sin(2\theta)\right]. \qquad (4\text{-}8)$$

In (4-8), the prime denotes differentiation with respect to x, and (0) is written for the point $(x,y)=(0,0)$.

The characteristic currents are determined by solving the matrix eigenvalue equation (2-33). Since the slot is narrow, however, partitioning of it is not necessary. The lkth elements of $\bar{\bar{G}}$ and $\bar{\bar{B}}$ then become

$$G_{ik} = \frac{1}{k\eta} \int_{-w}^{+w} f_i(x)\, dx$$

$$\left(\frac{d^2}{dx^2} + k^2\right) \int_{-w}^{+w} f_k(x') \left[1 - \frac{k^2}{4}|x-x'|^2\right] dx'$$

(4-9)

$$B_{ik} = \frac{-2}{\pi k\eta} \int_{-w}^{+w} f_i(x)\, dx$$

$$\left(\frac{d^2}{dx^2} + k^2\right) \int_{-w}^{+w} f_k(x') \log\left[\frac{\gamma k}{2}|x-x'|\right] dx'$$

An appropriate choice of f that satisfies the edge requirements indicated in Section 2-2, and is compatible with (4-8), is

$$f_k(x) = x^{k-1}\sqrt{w^2 - x^2} \qquad k=1,2 \qquad (4\text{-}10)$$

which results in a second order matrix eigenvalue equation. Substituting (4-10) into (4-9), and using the identities

$$\int_{-w}^{+w} \sqrt{w^2 - x^2}\, dx = w^2\pi/2$$

$$\int_{-w}^{+w} x^{2n-1} \sqrt{w^2 - x^2}\, dx = 0 \qquad (4\text{-}11)$$

$$n>0$$

$$\int_{-w}^{+w} x^{2n} \sqrt{w^2 - x^2}\, dx = \frac{(2n-1)!}{(n+1)!(n-1)!} \frac{w^{2(n+1)}\pi}{2^{2n}}$$

and [10, Appendix]

$$\int_{-w}^{+w} \sqrt{w^2 - x'^2} \log\left[\frac{\gamma k}{2} |x-x'|\right] dx' = \frac{w^2\pi}{2} \log\left[\frac{\gamma k w}{4}\right] + \frac{w^2\pi}{4}\left[2(x/w)^2 - 1\right] \qquad (4\text{-}12)$$

$$\int_{-w}^{+w} U_n(x'/w) \sqrt{w^2 - x'^2} \log\left[\frac{\gamma k}{2}|x-x'|\right] dx' =$$

$$-\frac{w^2\pi}{n(n+2)}\left[n\left[1 - (x/w)^2\right] U_n(x/w) + T_n(x/w)\right] \qquad n>0$$

where T_n and U_n are, respectively, the Chebyshev polynomials of the first and second kinds, (2-33) then becomes

$$-\frac{w^2\pi}{2}\begin{bmatrix} 2-(kw/2)^2+(kw)^2\log\left[\frac{\gamma kw}{4}\right] & 0 \\ 0 & w^2\left[1-\frac{2}{3}(kw/2)^2\right]\end{bmatrix}\begin{bmatrix}U_{n1}\\ U_{n2}\end{bmatrix}$$

$$= b_n\frac{w^2\pi^2}{2}\begin{bmatrix}(kw/2)^2\left[1-(kw/2)^2\right] & 0\\ 0 & (w/2)^2(kw/2)^4\end{bmatrix}\begin{bmatrix}U_{n1}\\ U_{n2}\end{bmatrix}. \qquad n=1,2$$

(4-13)

By inspection

$$b_1 = \frac{-1}{\pi(kw/2)^2[1-(kw/2)^2]}\left[2-(kw/2)^2+(kw)^2\log\left[\frac{\gamma kw}{4}\right]\right]$$

(4-14)

$$M_1(x) = C\sqrt{w^2-x^2}$$

and

$$b_2 = \frac{-4}{\pi(kw/2)^4}\left[1-\frac{2}{3}(kw/2)^2\right]$$

(4-15)

$$M_2(x) = Dx\sqrt{w^2-x^2}$$

are the solution-pairs of (4-13). As can be seen, b_1 and b_2 are very large negative numbers. Furthermore, since $2kw<<1$, the characteristic values are well approximated by

$$b_1 = -\frac{4}{\pi(kw)^2}\left[2 + (kw)^2 \log\left[\frac{\gamma kw}{4}\right]\right]$$

$$b_2 = -\frac{64}{\pi(kw)^4}. \qquad (4\text{-}16)$$

Consequently, to this approximation, the characteristic currents are given by

$$M_1(x) = \frac{2\sqrt{2\eta k}}{kw^2\pi}\sqrt{w^2 - x^2}$$

$$M_2(x) = \frac{8\sqrt{2\eta k}}{k^2w^4\pi}\, x\, \sqrt{w^2 - x^2} \qquad (4\text{-}17)$$

when normalized according to (2-36).

The equivalent magnetic current on the slot is given by

$$M(x) = \frac{\langle M_1, I\rangle}{1 + jb_1} M_1 + \frac{\langle M_2, I\rangle}{1 + jb_2} M_2$$

$$\approx \frac{\langle M_1,\ I\rangle}{1 + jb_1} M_1 - j\frac{\langle M_2,\ I\rangle}{b_2} M_2$$

$$\approx \eta k\left[\frac{H^{(2)}(0)}{\pi(kw/2)^2 - j(2 + (kw)^2\log(\gamma kw/4))} + \frac{j}{4} H^{(2)'}(0)\ x\right] \sqrt{w^2 - x^2}. \quad (4\text{-}18)$$

The magnetic current (4-18) reduces to that in [10] when all terms containing kw factors are ignored. Higher order solutions can be obtained by retaining more terms in (3-10) and using more expansion functions.

4-3 Evaluation of the Matrices $\bar{\bar{G}}$ and $\bar{\bar{B}}$

The general slot of arbitrary width can be solved using the Galerkin procedure of Section 2-6. Similar to the TE case, an efficient evaluation of the matrices $\bar{\bar{G}}$ and $\bar{\bar{B}}$ is essential for the success of the solution.

Because of the form of the operators G and B, a triangular expansion of the characteristic currents (see Figure 4-2) is attempted. This has the advantage of reducing the second order partial derivatives to finite differences [24], as well as approaching zero as $x \rightarrow \pm w$, although not at the rate specified by the edge conditions.

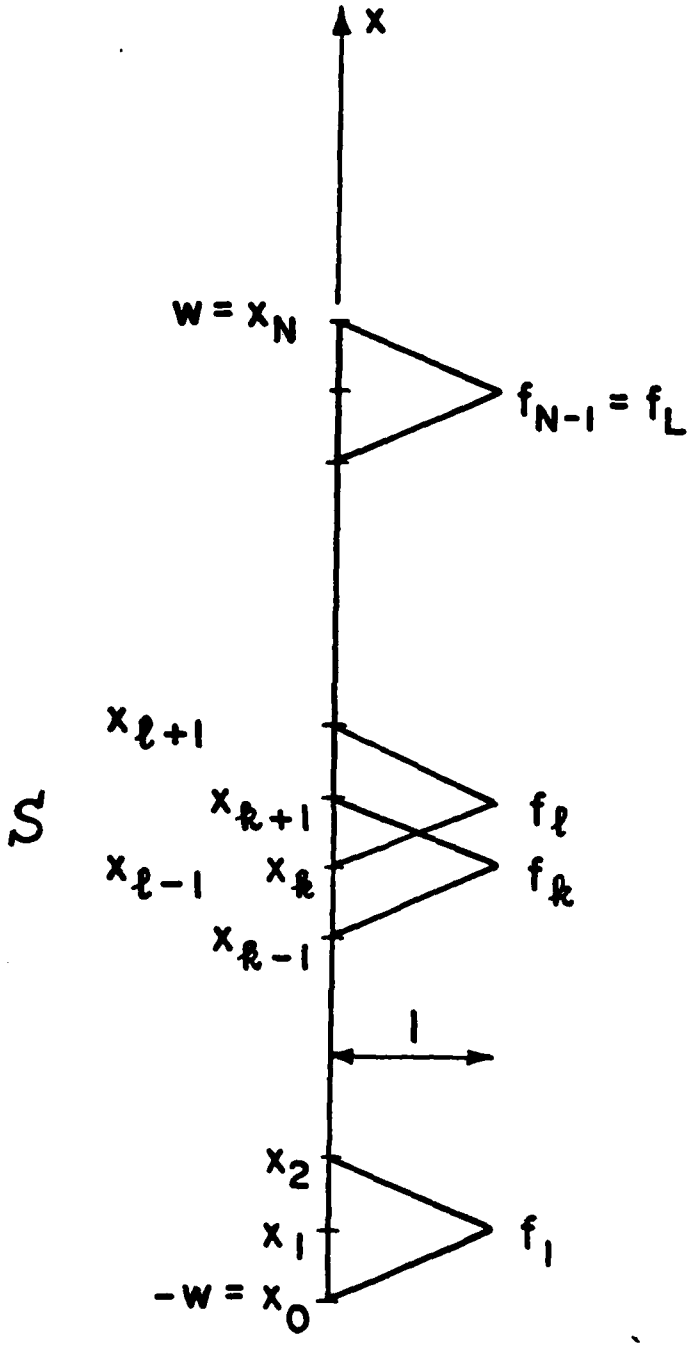

Figure 4-2. The triangular expansion functions for the characteristic currents.

To keep the notation simple, a uniform partition of the slot is assumed. Thus

$$f_k(x) = \frac{1}{S} \begin{cases} x - x_{k-1} & x_{k-1} \le x \le x_k \\ x_{k+1} - x & x_k \le x \le x_{k+1} \end{cases} \tag{4-19}$$

where S is the uniform width of the partition. The lkth elements of $\bar{\bar{G}}$ and $\bar{\bar{B}}$ are then given by

$$k\eta G_{lk} = \int_{x_{l-1}}^{x_{l+1}} f_l(x) \left[\left(\frac{d^2}{dx^2} + k^2 \right) G_k(x) \right] dx$$

$$k\eta B_{lk} = -\int_{x_{l-1}}^{x_{l+1}} f_l(x) \left[\left(\frac{d^2}{dx^2} + k^2 \right) B_k(x) \right] dx \tag{4-20}$$

where

$$G_k(x) = \int_{x_{k-1}}^{x_{k+1}} f_k(x') \, J_0(k|x-x'|) \, dx'$$

$$B_k(x) = \int_{x_{k-1}}^{x_{k+1}} f_k(x') \, N_0(k|x-x'|) \, dx' \tag{4-21}$$

Integrating the first term in (4-20) by parts twice, and approximating $G_k(x)$ by $G_k(x_i)$ and $B_k(x)$ by $B_k(x_i)$ in the second term, G_{ik} and B_{ik} then become

$$k\eta G_{ik} = \frac{1}{S}\left[G_k(x_{i+1}) - 2G_k(x_i) + G_k(x_{i-1})\right] + k^2 G_k(x_i)\int_{x_{i-1}}^{x_{i+1}} f_i(x)\,dx \tag{4-22}$$

$$k\eta B_{ik} = -\frac{1}{S}\left[B_k(x_{i+1}) - 2B_k(x_i) + B_k(x_{i-1})\right] - k^2 B_k(x_i)\int_{x_{i-1}}^{x_{i+1}} f_i(x)\,dx.$$

Since

$$\int_{x_{i-1}}^{x_{i+1}} f_i(x)\,dx = S, \tag{4-23}$$

the elements G_{ik} and B_{ik} of the matrices $\bar{\bar{G}}$ and $\bar{\bar{B}}$ become

$$k\eta G_{ik} = \frac{1}{S}\left[G_k(x_{i+1}) - 2(1-r)G_k(x_i) + G_k(x_{i-1})\right] \tag{4-24}$$

$$k\eta B_{ik} = -\frac{1}{S}\left[B_k(x_{i+1}) - 2(1-r)B_k(x_i) + B_k(x_{i-1})\right]$$

where $r=(k^2S^2/2)$. The evaluation of G_{1k} and B_{1k} ($|1-k|>2$) is then completed by performing the integrations in (4-21) numerically to obtain $G_k(x)$ and $B_k(x)$ at x_{1-1}, x_1, and x_{1+1}, and, for that purpose, any quadrature rule can be used.

When evaluating the diagonal and the first and second lower and upper diagonal elements of $\bar{\bar{B}}$, B_{1k}, $|1-k|\leq 2$, singularities are encountered. As has been seen in the TE case, this situation is best dealt with by integrating the singular part of the integrand analytically. The non-singular remainder is then integrated numerically using a quadrature formula. Thus

$$B_k(x_j) = \overset{p}{B}_k(x_j) + \overset{s}{B}_k(x_j)$$

where

$$\overset{p}{B}_k(x_j) = \int_{x_{k-1}}^{x_{k+1}} f_k(x')\, N_{op}(k|x_j-x'|)\, dx'$$

and

$$\overset{s}{B}_k(x_j) = \int_{x_{k-1}}^{x_{k+1}} f_k(x')\, N_{os}(k|x_j-x'|)\, dx' \qquad (4\text{-}25)$$

where N_{os} is the small argument approximation of N_o given

by (3-10), $N_{op} = N_o - N_{om}$, and $j \in \{k-1, k, k+1\}$. The integration in (4-25) is readily performed as

$$B_k^s(x_j) = \frac{2}{\pi S} \sum_{\substack{i=k-1,\\ k+1}} \int_{x_i}^{x_k} (x' - x_i) \log\left[\frac{\gamma_k}{2}|x_j - x'|\right] dx'$$

$$= \frac{2}{\pi S} \sum_{\substack{i=k-1,\\ k+1}} \int_{x_j - x_i}^{x_j - x_k} (u - (x_j - x_i)) \log\left|\frac{\gamma_k}{2} u\right| du$$

$$= \frac{1}{\pi S} \sum_{\substack{i=k-1,\\ k+1}} \left[|x_j - x_k|^2 \left[\log\left[\frac{\gamma_k}{2}|x_j - x_k|\right] - \frac{1}{2}\right] \right.$$

$$- 2|x_j - x_i||x_j - x_k| \left[\log\left[\frac{\gamma_k}{2}|x_j - x_k|\right] - 1 \right]$$

$$\left. + |x_j - x_i|^2 \left[\log\left[\frac{\gamma_k}{2}|x_j - x_i|\right] - \frac{3}{2}\right] \right]. \qquad (4\text{-}26)$$

In obtaining (4-26), advantage was taken of the non-negative nature of $(x_j - x_i)(x_j - x_k)$ to replace it by its absolute value. Since

$$x_j = -w + jS \qquad (4\text{-}27)$$

then

$$B_k^s(x_j) = \frac{S}{\pi} \sum_{\substack{i=k-1,\\ k+1}} \left[|j-k|^2 \left[\log\left[\frac{\gamma k}{2}|j-k|S\right] - \frac{1}{2}\right] \right.$$

$$- 2|j-i||j-k|\left[\log\left[\frac{\gamma k}{2}|j-k|S\right] - 1\right]$$

$$\left. + |j-i|^2 \left[\log\left[\frac{\gamma k}{2}|j-i|S\right] - \frac{3}{2}\right]\right]. \qquad (4\text{-}28)$$

When $|j-k|=1$, $B_k^s(x_j)$ of (4-28) reduces to β_1 and when $j=k$, $B_k^s(x_j)$ reduces to β_2 where

$$\beta_1 = \frac{S}{\pi}\left[2\log\left[2\gamma kS\right] - 3\right] \qquad (4\text{-}29)$$

$$\beta_2 = \frac{S}{\pi}\left[2\log\left[\frac{\gamma k}{2}S\right] - 3\right].$$

The quantities $(B_k(x_j), j=l-1, l, l+1)$ appear on the right-hand side of the second of equations (4-24).

Retaining (4-24) whenever $|k-1|>2$, and replacing $B_k(x_j)$ by means of (4-25) and (4-29) whenever $|j-k|\leq 1$, we obtain

$$k\eta G_{1k} = \frac{1}{s}\left[G_k(x_{1+1}) - 2(1-\Gamma)G_k(x_1) + G_k(x_{1-1})\right] \quad \text{for all } 1,k$$

$$k\eta B_{1k} = \begin{cases} -\frac{1}{s}\left[B_k(x_{1+1}) - 2(1-\Gamma)B_k(x_1) + B_k(x_{1-1})\right] & \text{if } |k-1|>2 \\ -\frac{1}{s}\left[\overset{p}{B}_k(x_{1+1}) - 2(1-\Gamma)B_k(x_1) + B_k(x_{1-1}) + \beta_1\right] & \text{if } k-1=2 \\ -\frac{1}{s}\left[B_k(x_{1+1}) - 2(1-\Gamma)B_k(x_1) + \overset{p}{B}_k(x_{1-1}) + \beta_1\right] & \text{if } 1-k=2 \\ -\frac{1}{s}\left[\overset{p}{B}_k(x_{1+1}) - 2(1-\Gamma)\overset{p}{B}_k(x_1) + B_k(x_{1-1}) + \beta_2 - 2(1-\Gamma)\beta_1\right] & \text{if } k-1=1 \\ -\frac{1}{s}\left[B_k(x_{1+1}) - 2(1-\Gamma)\overset{p}{B}_k(x_1) + \overset{p}{B}_k(x_{1-1}) + \beta_2 - 2(1-\Gamma)\beta_1\right] & \text{if } 1-k=1 \\ -\frac{1}{s}\left[\overset{p}{B}_k(x_{1+1}) - 2(1-\Gamma)\overset{p}{B}_k(x_1) + \overset{p}{B}_k(x_{1-1}) + 2\beta_1 - 2(1-\Gamma)\beta_2\right] & \text{if } 1=k. \end{cases}$$

(4-30)

In (4-30), $B_k^p(x_j)$, $j \in \{k-1, k, k+1\}$, is evaluated as

$$B_k^p(x_j) \approx S \sum_{n=1}^{Q} c_n f_k(x_k+d_nS) N_{op}(k|x_j-(x_k+d_nS)|) \tag{4-31}$$

where Q is the order, c_n are the coefficients, and d_n are the abscissas of the quadrature rule.

4-4 Numerical Results

The characteristic currents and electric fields as well as the equivalent magnetic current and radiation pattern have been computed for different slot widths. Some of the results obtained for the 0.4λ, 0.5λ, and 1.0 λ slots are given in this section.

In the actual computation, polynomial approximations of the Bessel functions J_o and N_o [22, Articles 9.4.1-9.4.3] are utilized, while all the integrals are computed using an eight-point Gaussian quadrature [22, Table 25.4]. The characteristic electric fields E_{ny} are given by

$$E_{ny} = \frac{\pm 1}{j2} \int_{-w}^{+w} \frac{kz}{\sqrt{z^2+(x-x')^2}} M_n(x') H_1^{(2)}\left(k\sqrt{z^2+(x-x')^2}\right) dx' \tag{4-32}$$

where $H_1^{(2)}$ is the Hankel function of second kind and first order. The upper sign is used for $z<o$ and the lower one for $z>0$. The far fields can then be obtained by replacing the Hankel function by its large argument approximation [9, Appendix D]:

$$H_1^{(2)}(s) = j\sqrt{2j/(\pi s)}\, e^{-js} \tag{4-33}$$

and using the radiation zone approximations (3-39). Thus, substituting (2-28) for M_n with $f_k(x)$ given by (4-19), we obtain

$$E_{ny} \approx \pm \frac{1+j}{2} \sqrt{k/(\pi r)}\, \sin\phi \left[\frac{\sin((kS\cos\phi)/2)}{(kS\cos\phi)/2}\right]^2 S\, e^{-jkr} \sum_{k=1}^{L} U_{nk}\, e^{jkx_k\cos\phi}$$

$$= A(r,\phi) \sum_{k=1}^{L} U_{nk}\, e^{jkx_k\cos\phi} \tag{4-34}$$

at any point $(r,\phi)\in C_{yr}$ when $r>>2w$ and $kr>>1$. In (4-34), ϕ is the angle $\underline{r}=x\underline{u}_x+z\underline{u}_z$ makes with the x-axis.

All the features and convergence patterns found for the TE case are repeated for the TM case. The convergence of the characteristic values is monotone, either upward or downward, as can readily be seen in Tables 4-1, 4-2, and 4-

Table 4-1

The convergence of the characteristic values for the 0.4λ slot.

	L	b_1	b_2	b_3	b_4	...
	4	-0.9704768	-39.8842620	-3720.14844	∞	∗
	8	-0.9579801	-35.8596497	-2545.51025	-411088.187	∞
	12	-0.9465772	-34.6101685	-2324.73218	-369193.812	∞
	16	-0.9390166	-33.9757080	-2227.90527	-269168.375	∞
	20	-0.9338933	-33.5944824	-2185.04346	-265509.875	∞
→	24	-0.9298853	-33.3237762	-2155.04395	-237685.375	∞

Table 4-2

The convergence of the characteristic values for the 0.5 λ slot.

	L	b_1	b_2	b_3	b_4	...
	4	-0.4591318	-14.9436836	-897.567627	∞	∗
	8	-0.4725091	-14.0017996	-648.799561	-62683.6680	∞
	12	-0.4709589	-13.6431913	-600.401367	-51791.5703	∞
	16	-0.4687450	-13.4430857	-579.949951	-49074.1836	∞
	20	-0.4668146	-13.3114119	-567.934814	-47766.3203	∞
	24	-0.4653491	-13.2199717	-560.609375	-48250.5898	∞
→	28	-0.4641726	-13.1521626	-555.927002	-49039.1602	∞

Table 4-3

The convergence of the characteristic values for the 1.0 λ slot.

L	b_1	b_2	b_3	b_4	b_5
4	0.007760	-0.2222299	-6.3792248	-316.052002	*
8	-0.0100392	-0.4589630	-7.8628264	-187.909714	-8264.32031
12	-0.0139949	-0.5044749	-8.1955252	-179.558655	-6616.984337
16	-0.0157180	-0.5185139	-8.2802639	-176.418991	-6160.37109
20	-0.0167178	-0.5237506	-8.2951450	-174.405258	-5933.50781
24	-0.0173952	-0.5258325	-8.2879648	-172.971313	-5828.77734
28	-0.0178963	-0.5265995	-8.2730077	-171.782654	-5732.35547
32	-0.0182855	-0.5267935	-8.2571888	-170.876831	-5652.25781
36	-0.0185869	-0.5265971	-8.2394047	-170.050171	-5601.01953
→ 40	-0.0188513	-0.5263984	-8.2251053	-169.446167	-5562.56641

3. It should be noted, however, that only four characteristic modes for the 0.4λ and 0.5λ slots and five for the 1.0λ slot are computed compared, respectively, to five and seven for the TE case. This is because the corresponding programs were run on different computers having different computing precisions. When the TE program was run in the new computing environment, there resulted the same number of significant modes. The characteristic currents and far electric fields for the slots considered are shown in Figures 4-3, 4-5, 4-7, 4-9, 4-11, and 4-13. Figures 4-5, 4-9, and 4-13 are polar plots. The curve of the characteristic current $M_4(x)$ in Figure 4-3 is not exactly odd about x=0 because of roundoff error. The corresponding equivalent magnetic currents and radiation patterns are shown in Figures 4-4, 4-6, 4-8, 4-10, 4-12, and 4-14. Figures 4-6, 4-10, and 4-14 are polar plots. When a slot is excited by the plane wave (4-1) with $\theta=0°$, the equivalent magnetic current $\underline{M}$ is given by (2-15). Table 4-4 gives for each slot the ratio of the power radiated by each characteristic current $V_n\underline{M}_n$ in (2-15) to that radiated by the dominant characteristic current $V_1\underline{M}_1$. All data are evaluated with L as specified in the arrow marked rows in Tables 4-1, 4-2, and 4-3.

Table 4-4

The ratio of the power radiated by each characteristic current to that radiated by the dominant characteristic current for a (a) 0.4 λ slot, (b) 0.5 λ slot, and (c) 1.0 λ slot.

(a)

n	P_n / P_1
1	1.0
2	0.100758
3	0.251782×10^{-2}
4	0.1633407×10^{-4}
...	0.0

(b)

n	P_n / P_1
1	1.0
2	0.161499
3	0.6648028×10^{-2}
4	0.7618671×10^{-4}
...	0.0

(c)

n	P_n/P_1
1	1.0
2	0.062435
3	0.012813
4	0.105344×10^{-2}
5	0.349562×10^{-4}
...	0.0

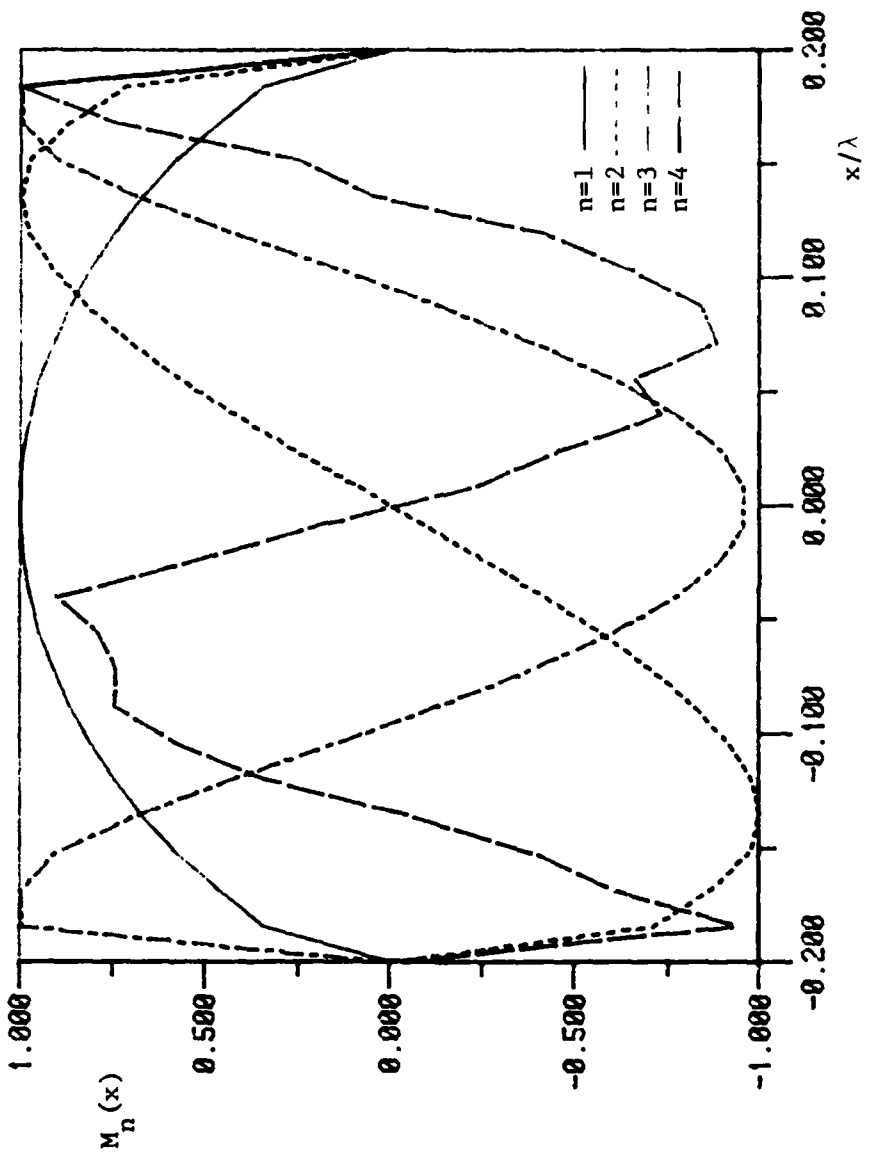

Figure 4-3. The first 4 characteristic currents for the 0.4λ slot.

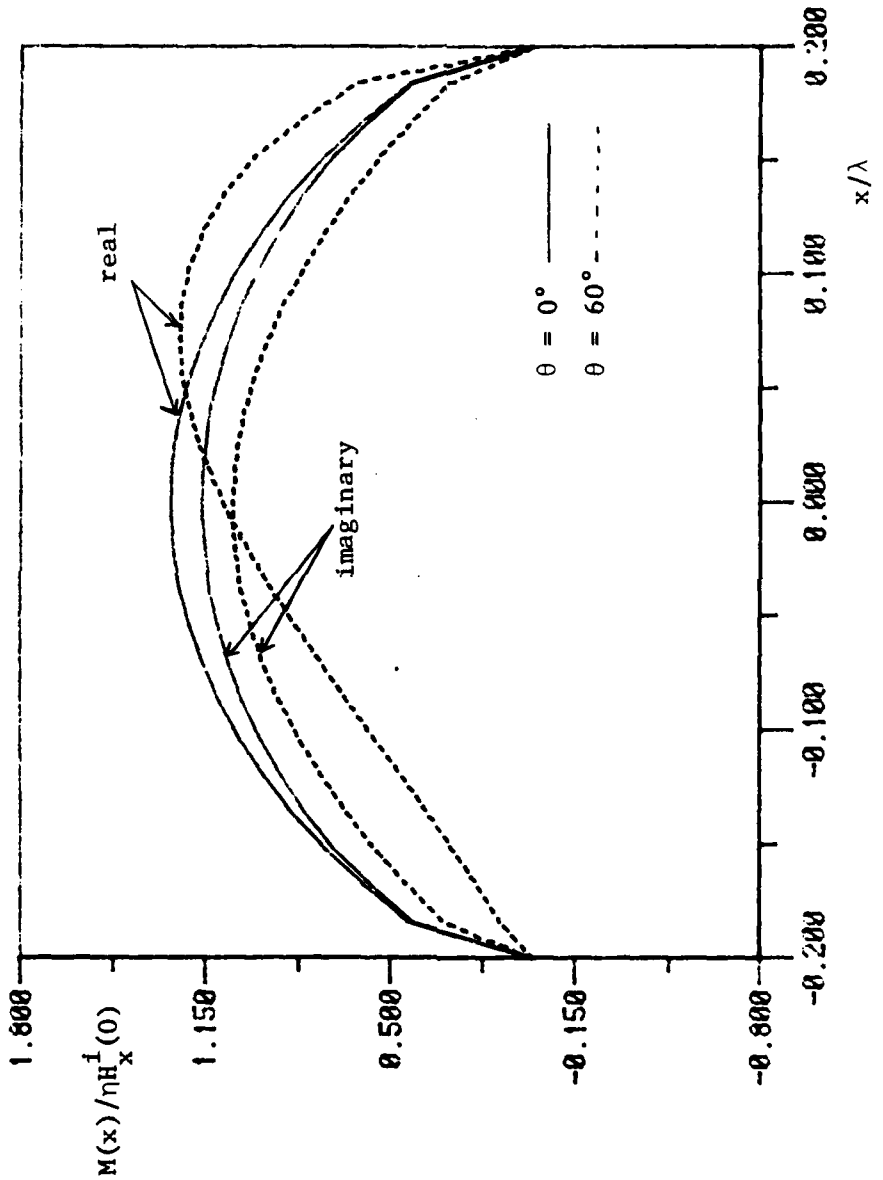

Figure 4-4. The equivalent magnetic current for the 0.4λ slot.

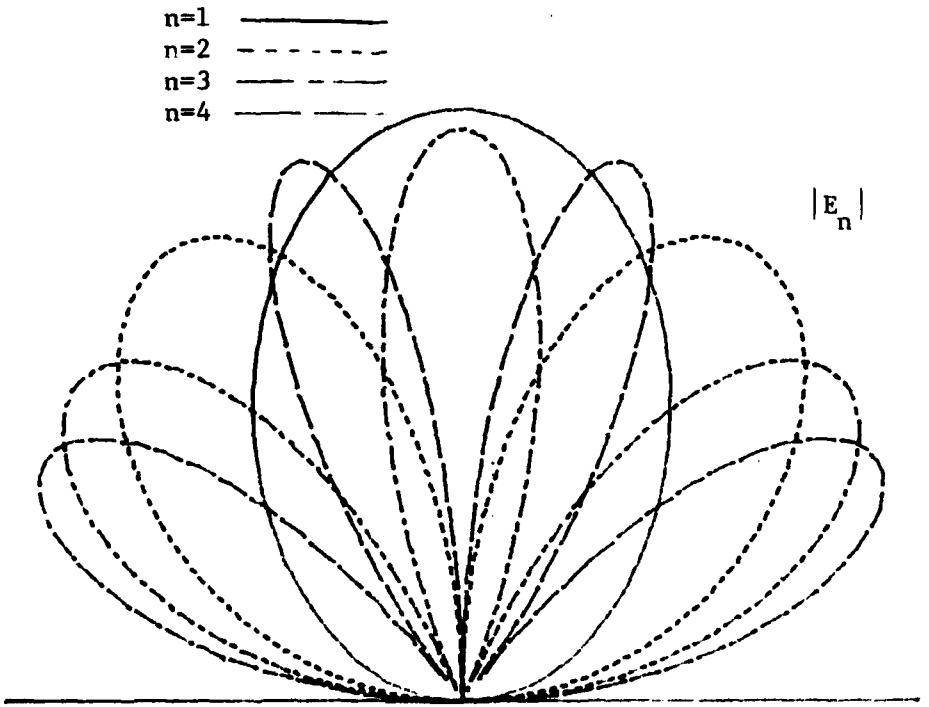

Figure 4-5. The radiation patterns for the first 4 characteristic electric fields for the 0.4λ slot.

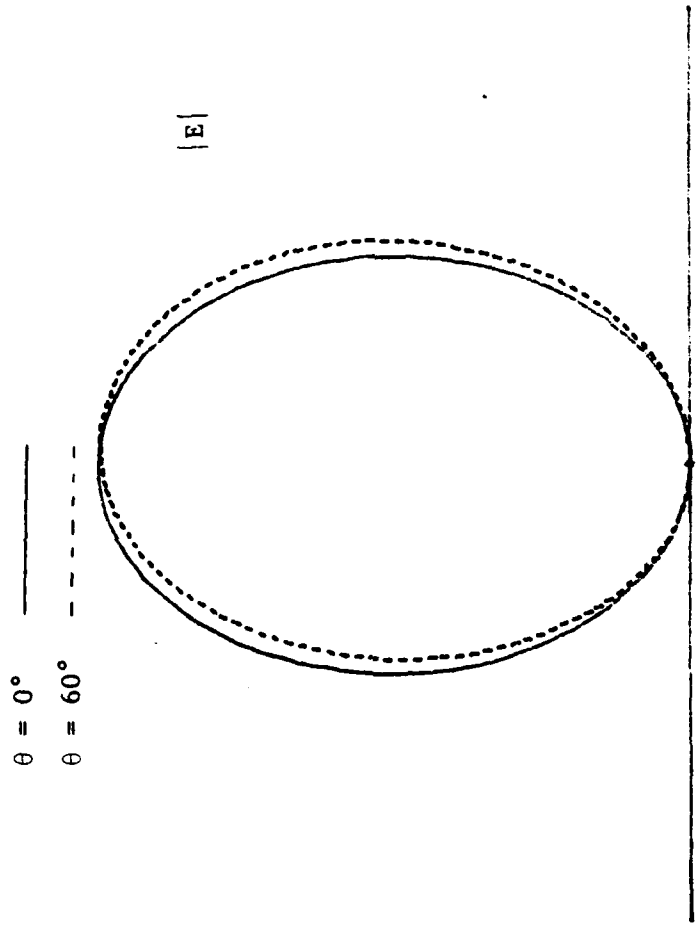

Figure 4-6. The radiation pattern for the 0.4λ slot.

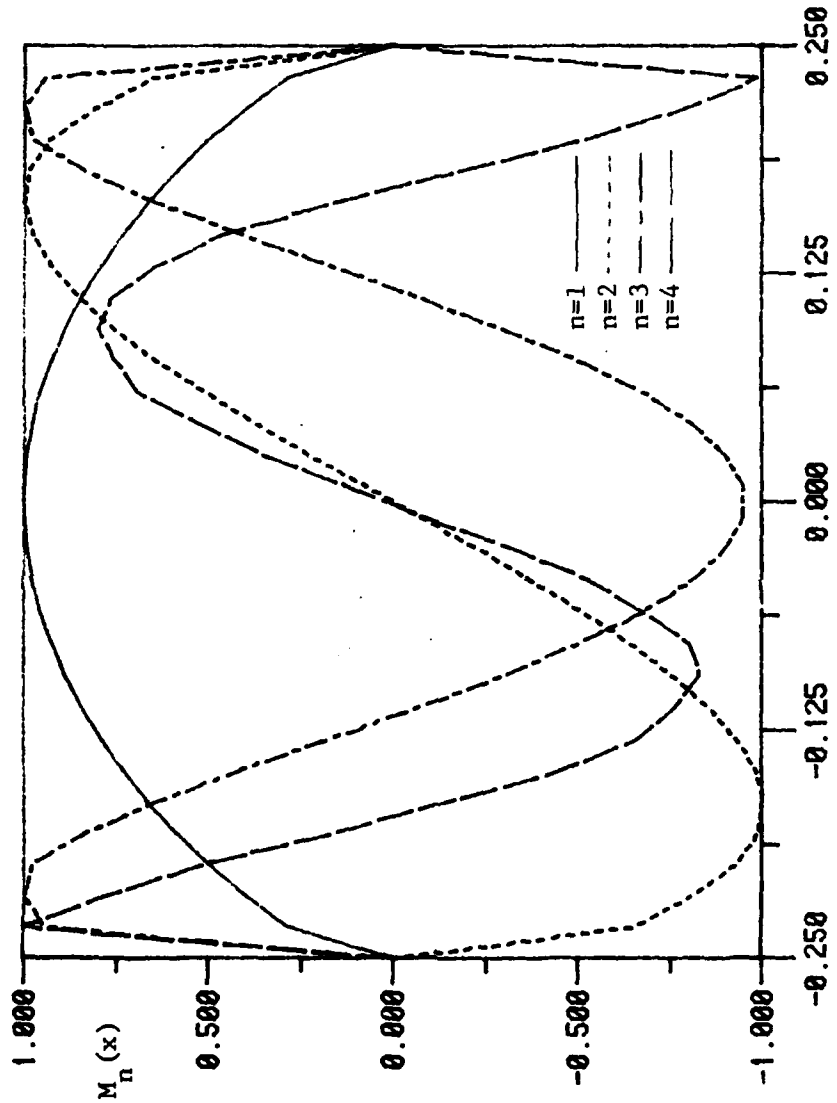

Figure 4-7. The first 4 characteristic currents for the 0.5λ slot.

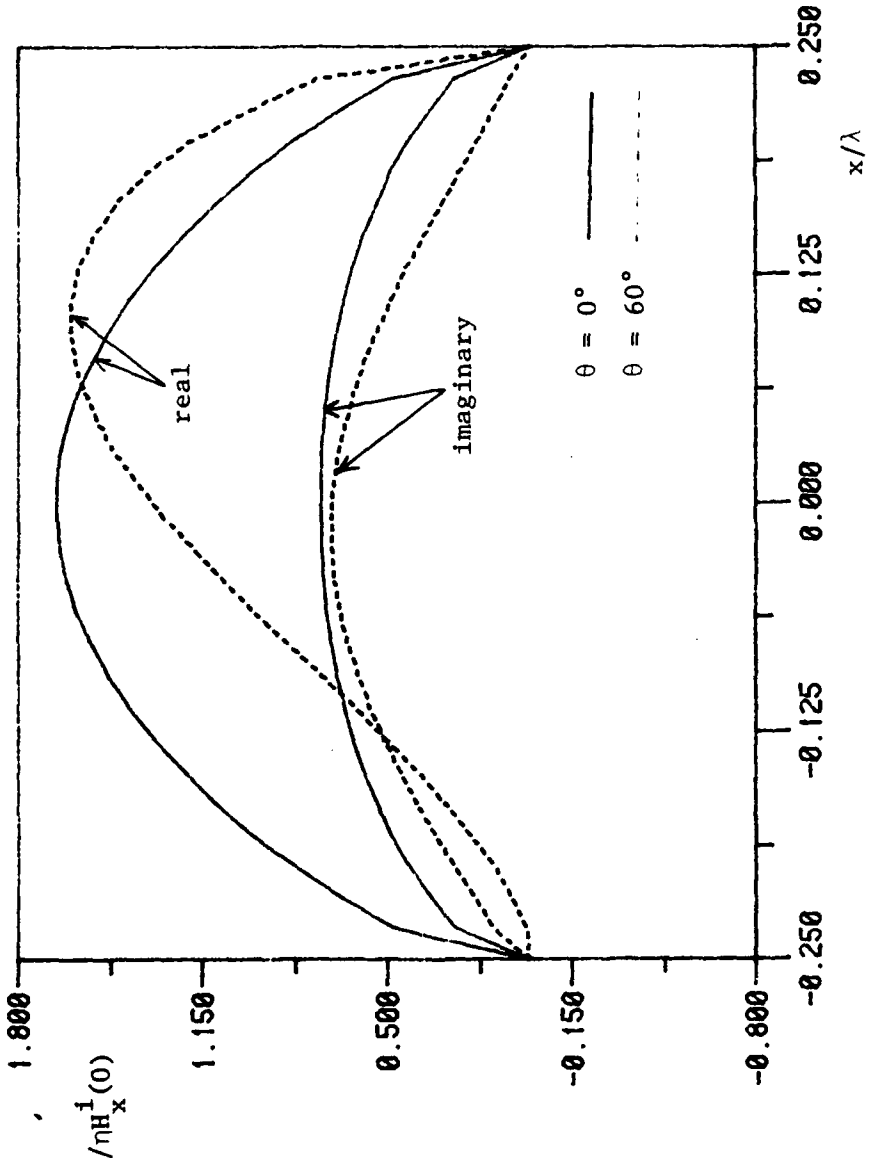

Figure 4-8. The equivalent magnetic current for the 0.5λ slot.

AD-A163 523 CHARACTERISTIC MODES FOR A SLOT IN A CONDUCTING PLANE (U) SYRACUSE UNIV NY DEPT OF ELECTRICAL AND COMPUTER ENGINEERING K Y KABALAN ET AL DEC 85 SYRU/DECE/TR85/6 2/2

UNCLASSIFIED N00014-85-K-0082 F/G 20/3 NL

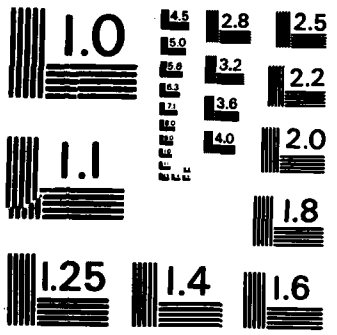

MICROCOPY RESOLUTION TEST CHART
NATIONAL BUREAU OF STANDARDS-1963-A

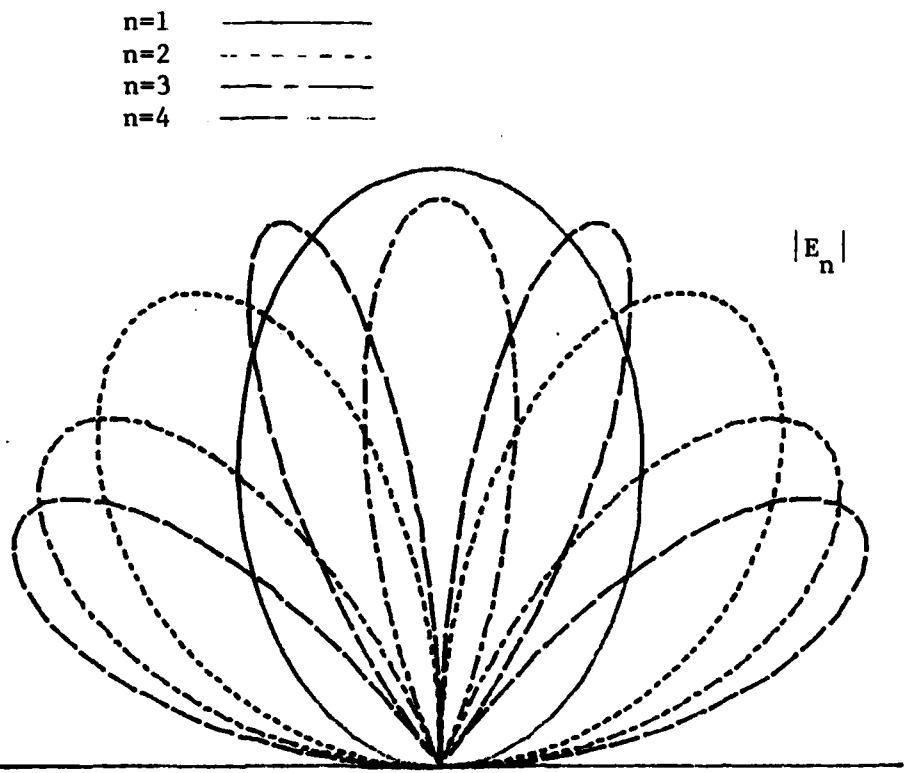

Figure 4-9. The radiation patterns for the first 4 characteristic electric fields for the 0.5λ slot.

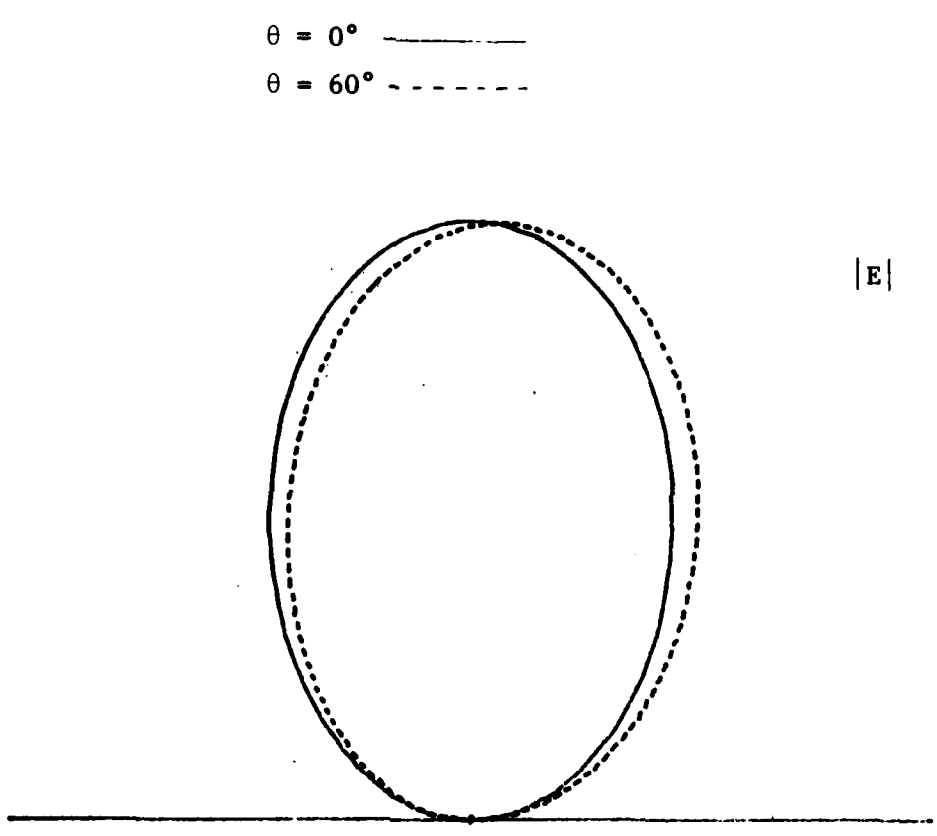

Figure 4-10. The radiation pattern for the 0.5λ slot.

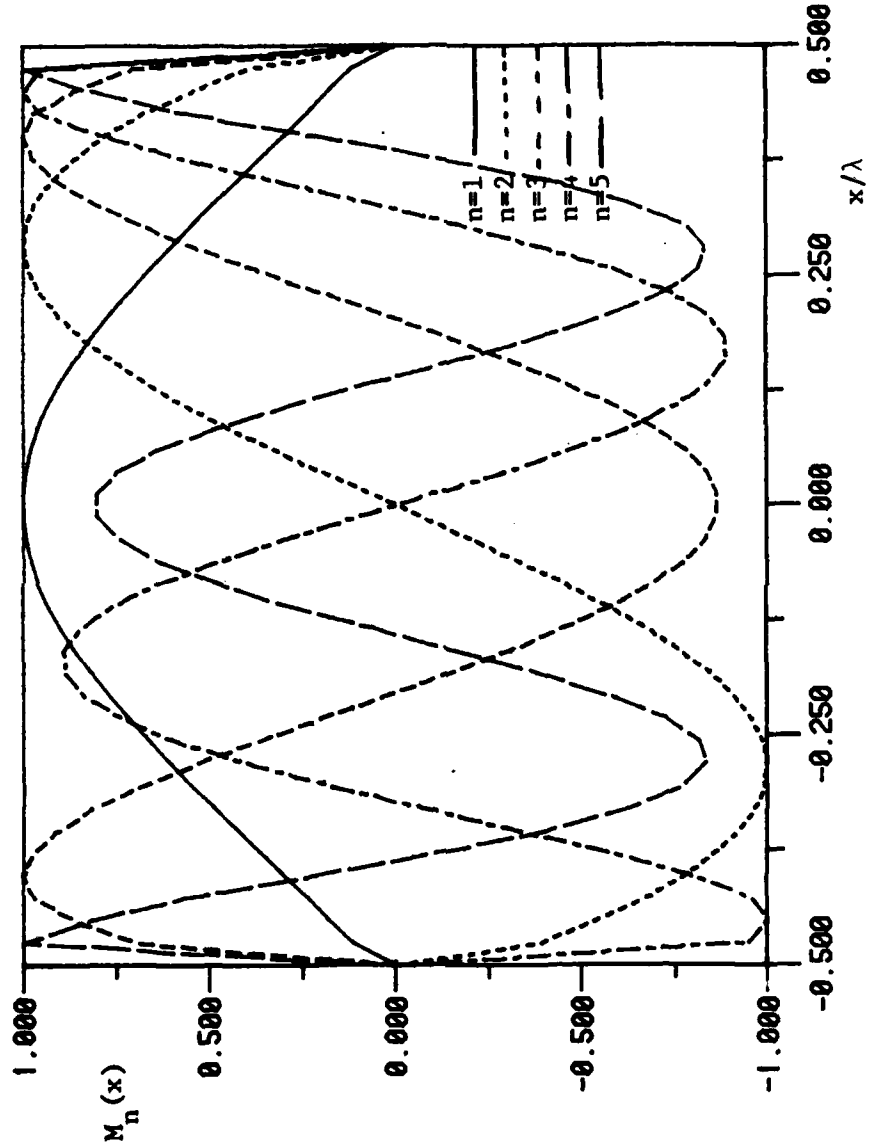

Figure 4-11. The first 5 characteristic currents for the 1.0λ slot.

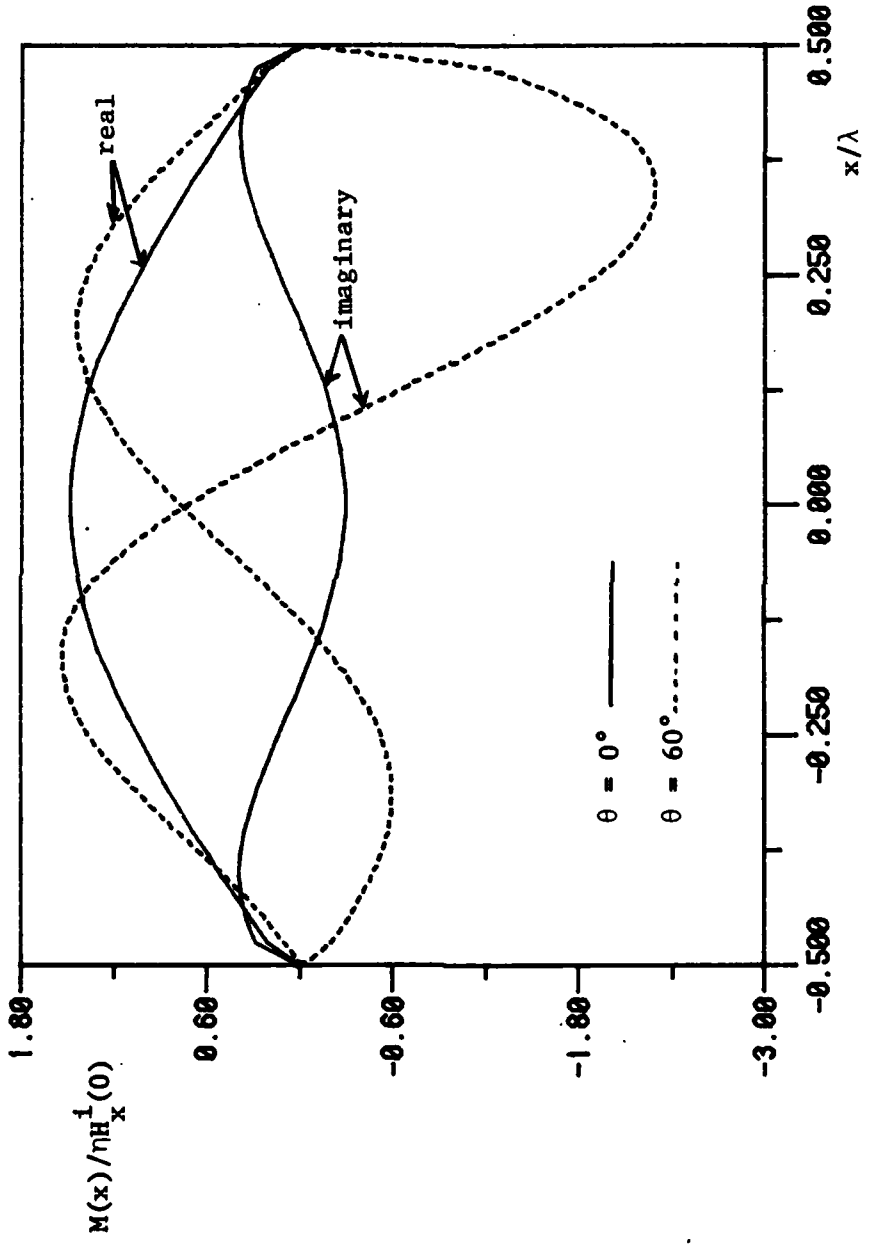

Figure 4-12. The equivalent magnetic current for the 1.0λ slot.

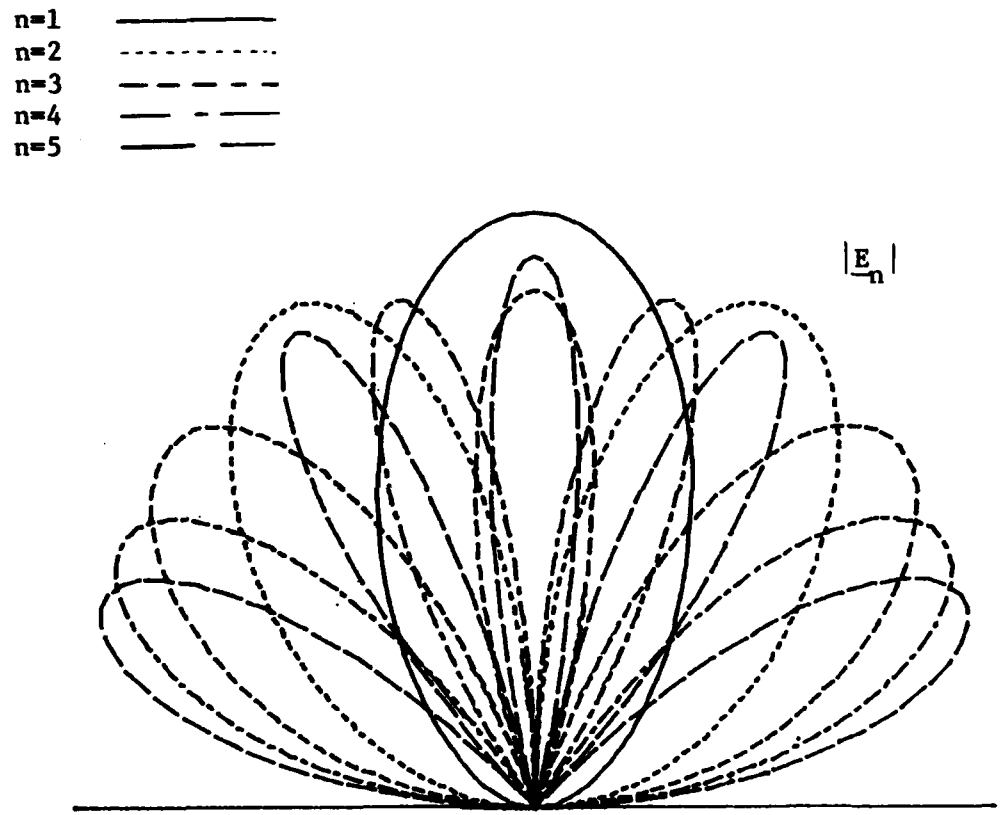

Figure 4-13. The radiation patterns for the first 5 characteristic electric fields for the 1.0λ slot.

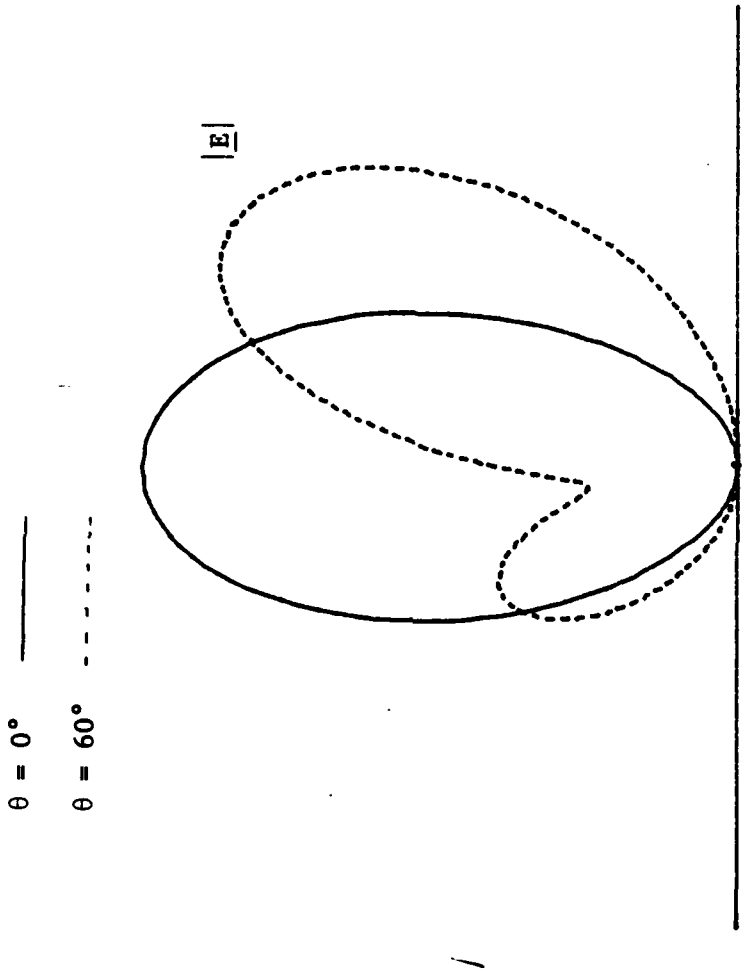

Figure 4-14. The radiation pattern for the 1.0λ slot.

CHAPTER 5

DISCUSSION

The theory of characteristic modes for slots has been applied to the solution of the problem of an infinitely long slot in a ground plane illuminated by either a transverse electric or a transverse magnetic plane wave. The theory is a specialization of the general theory of characteristic modes for apertures, and can be applied to slots in a conducting plane separating contrasting mediums and illuminated by a general wave.

Some conclusions are drawn from the application of the theory in the report.

1- The theory is equally applicable to narrow as well as to general slots.

2- The theory results in a modal expansion for all quantities and parameters of interest usually encountered in electromagnetic compatibility problems, such as the equivalent magnetic current on the slot, the transmission coefficient, and the radiation pattern.

3- For narrow slots, the theory reduces to an augmented Bethe theory, i.e., the slot is represented by a susceptance term related to the polarizability, plus a conductance term.

4- Only a finite number of characteristic currents and field modes need to be computed for a slot of arbitrary width.

5- When the slot is narrow, only a few terms are needed in the modal expansion mentioned in 2 above.

Although the presentation is confined to a slot in a conducting plane in an unbounded medium, the conclusions drawn above are expected to hold for a slot in a conducting plane separating mediums with different electromagnetic properties. The extension to the two-medium problem can be accomplished in a straightforward manner. The application of the theory to another kind of aperture like the circular or elliptic aperture, or for that matter a general aperture of arbitrary shape, however, is a major task worthy of consideration. The study of the transmission of electromagnetic energy through apertures backed by resonant cavities, or loaded by dielectric sheaths or strips is of both theoretical and practical importance. Other areas of possible study include phased array antennas, pattern synthesis, and supergain array design.

The theory of characteristic modes for apertures is versatile. It has been applied with great success to slots

in a conducting plane in the report, and promises equal success for other aperture problems.

Appendix A

In this Appendix, it is shown that the convergence of the modal expansion of $\underline{E}(\underline{M})$ is in a least squares sense over the radiation cylinder. The proof for $\underline{H}(\underline{M})$ is similar. Let

$$\underline{E}^{(N)}(\underline{M}) = \sum_{n=1}^{N} V_n \underline{E}_n \tag{A-1}$$

be the N-term modal expansion of $\underline{E}(\underline{M})$ and let $\underline{E}(\underline{M})$ be the quantity toward which it converges.

$$\underline{E}(\underline{M}) = \lim_{N\to\infty} \sum_{n=1}^{N} V_n \underline{E}_n \tag{A-2}$$

If

$$U_n = \lim_{N\to\infty} V_n \tag{A-3}$$

then

$$\underline{E}(\underline{M}) = \sum_{n=1}^{\infty} U_n \underline{E}_n . \tag{A-4}$$

The difference between (A-1) and (A-4) is called the residual $\underline{R}_N$.

$$\underline{R}_N = \sum_{n=1}^{\infty} U_n \underline{E}_n - \sum_{n=1}^{N} V_n \underline{E}_n \tag{A-5}$$

Then, the convergence of $\underline{E}(\underline{M})$ in a least squares sense over the radiation cylinder is equivalent to the requirement that the square of the norm of the residual

$$\|\underline{R}_N\|^2 = \int_{C_{ye}} \underline{R}_N^* \cdot \underline{R}_N \, d\tau \qquad (A-6)$$

be minimum. Substituting (A-5) into (A-6) and using the first orthogonality relationship of (2-25), there results

$$\|\underline{R}_N\|^2 = \eta \left[\sum_{n=1}^{N} |U_n - V_n|^2 + \sum_{n=N+1}^{\infty} |U_n|^2 \right]. \qquad (A-7)$$

The quantity (A-7) is minimum when

$$V_n = U_n \,, \quad n=1,2,\ldots,N \qquad (A-8)$$

As given by (2-19), V_n does not depend on N. It is now evident from (A-3) that V_n is given by (A-8). Therefore the modal coefficients V_n minimize (A-7) so that the convergence of the modal expansion of $\underline{E}(\underline{M})$ is in a least squares sense over the radiation cylinder.

References

[1] R. F. Harrington and J. R. Mautz, "A Generalized Network Formulation for Aperture Problems," IEEE Transactions on Antennas and Propagation, Volume AP-24, Pages 870-873, November 1976.

[2] R. F. Harrington and J. R. Mautz, "Characteristic Modes for Aperture Problems," IEEE Transactions on Microwave Theory and Techniques, Volume MTT-33, Pages 500-505, June 1985.

[3] Lord Rayleigh, "On the Passage of Waves through Apertures in Plane Screens, and Allied Problems," Philosophical Magazine, Series 5, Volume 43, Pages 259- 272, 1897.

[4] A. Sommerfeld, Optics, Lectures on Theoretical Physics, Volume IV, Academic Press, New York, New York, 1954.

[5] P. M. Morse and P. J. Rubenstein, "The Diffraction of Waves by Ribbons and by Slits," Physical Review, Volume 54, Pages 895-898, 1938.

[6] R. Barakat, "Diffraction of Plane Waves by a Slit between Two Different Media," Journal of the Optical Society of America, Volume 53, Pages 1231-1243, November 1963.

[7] R. F. Millar, "A Note on Diffraction by an Infinite Slit," Canadian Journal of Physics, Volume 38, Pages 38-47, 1960.

[8] K. Houlberg, "Diffraction by a Narrow Slit in the Interface between Two Different Media," Canadian Journal of Physics, Volume 45, Pages 57-81, 1967.

[9] R. F. Harrington, Time- Harmonic Electromagnetic Fields, McGraw-Hill Book Company, New York, New York, 1961.

[10] C. M. Butler and D. R. Wilton, "General Analysis of Narrow Strips and Slots," IEEE Transactions on Antennas and Propagation, Volume AP-28, Pages 42-48, January 1980.

[11] R. F. Harrington, Field Computation by Moment Methods, Macmillan Company, New York, New York, 1968. Reprinted by Krieger Publishing Company, Melbourne, Florida, 1982.

[12] C. M. Butler and K. R. Umashankar, "Electromagnetic Penetration through an Aperture in an Infinite, Planar Screen Separating Two Half Spaces of Different Electromagnetic Properties," Radio Science, Volume 11, Pages 611-619, July 1976.

[13] T. Y. Chou and A. T. Adams, "The Coupling of Electromagnetic Waves through Long Slots," IEEE Transactions on Electromagnetic Compatibility, Volume EMC-19, Pages 65-73, May 1977.

[14] G. C. Lewis,"A Numerical Solution for Electromagnetic Penetration through a Dielectric Sheath-Covered Slotted Screen," Master's Thesis, University of Mississippi, University, Mississippi, December 1976.

[15] R. D. Nevels and C. M. Butler, "Electromagnetic Diffraction by a Slot in a Ground Screen Covered by a Dielectric Slab," IEEE Transactions on Antennas and Propagation, Volume AP-30, Pages 390-395, May 1982.

[16] D. T. Auckland and R. F. Harrington, "Electromagnetic Transmission through a Filled Slit in a Conducting Plane of Finite Thickness, TE Case, " IEEE Transactions on Microwave Theory and Techniques, Volume MTT-26, Pages 499-505, July 1978.

[17] D. T. Auckland and R. F. Harrington, "Electromagnetic Transmission through Cascaded Rectangular Regions in a Thick Conducting Screen, "AEU, Volume 34, Pages 19-26, 1980.

[18] F. B. Hildebrand, Methods of Applied Mathematics, Prentice-Hall, Inc., Englewood Cliffs, New Jersey, 1965.

[19] R. E. Collin, Field Theory of Guided Waves, McGraw-Hill Book Company, New York, New York, 1960.

[20] R. F. Harrington and J. R. Mautz, "Theory of Characteristic Modes for Conducting Bodies," IEEE Transactions on Antennas and Propagation, Volume AP-19, Pages 622-628, September 1971.

[21] T. M. Apostol, Mathematical Analysis, Addison-Wesley Publishing Company, Reading, Massachusetts, 1957.

[22] M. Abramowitz and I. A. Stegun, Handbook of Mathematical Functions, Dover Publications, New York, New York, 1965.

[23] IMSL Library 2 Manual, 1975.

[24] D. R. Wilton and C. M. Butler, "Efficient Numerical Techniques for Solving Pocklington's Equation and Their Relationships to Other Methods," IEEE Transactions on Antennas and Propagation, Volume AP-24, Pages 83-86, January 1976.

END

FILMED

3 -86

DTIC